Graduation Thesis

P5 MARTIJN NIJKAMP
4660839

3D Printing in Construction

On the gap between innovation and practical use.

& Tesla valves as a passive regulating strategy for natural ventilation

First mentor
Dr.ing. M. Bilow
Second mentor
Ir. E.R. van den Ham

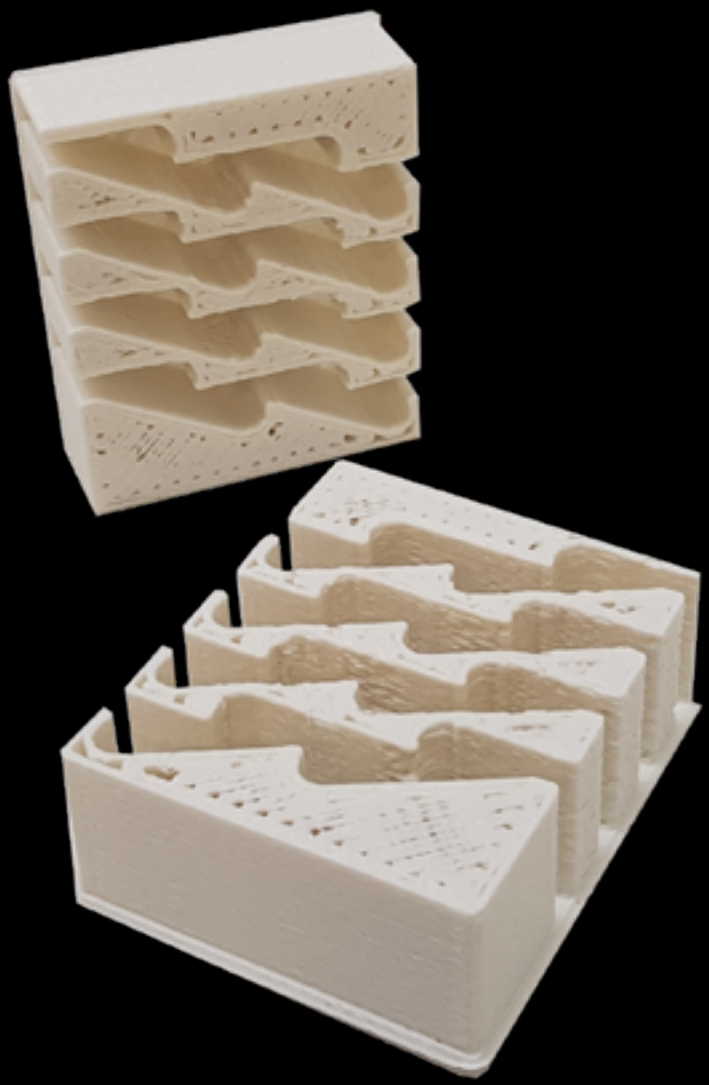

DELFT UNIVERSITY OF TECHNOLOGY
17/06/2024

Contents

Section 1

Additive Manufacturing in the built environment

Despite decades of development, large-scale 3D printing (3DP) has not found widespread application in the built environment (El-Sayegh et al., 2020), nor has it delivered any commercially available and widely used products within the construction industry (Rashid et al., 2020). Nonetheless, advancements towards adapting the technology are being made, with the bulk of innovation focusing on 3D concrete printing (3DCP) (Rashid et al., 2020). Although the potential of these advancements is significant (already entire buildings are being printed in a matter of days) (Weger et al., 2021), right now, the main motivators are economical in nature, resulting in an excessive focus on time and efficiency gains (Niaki et al., 2019). This leads to the major part of development being done on the 3DP technology itself, rather than on developing truly innovative new ways to design and construct, causing a continuation of the traditional construction and design practices. This is problematic not only because traditional ways of designing and constructing can be inefficient and its perpetuation stifles radical innovation (R. A. Buswell et al., 2007), but also because research is divided on the question if large-scale 3D printing will be either faster or cheaper when deployed to produce traditionally designed buildings and building components (Wu et al., 2016) (Yin et al., 2018). Instead, research suggests that to make large-scale adaptation 3DP possible, it should be used to facilitate a paradigm shift towards holistic (Jared et al., 2017), or free-form (R. Buswell et al., 2005) design, two concepts that describe the practice of enhancing building components efficiency or adding multiple functionalities through geometric complexity which, due to the way additive manufacturing works, does not add to production cost, which is often referred to as complexity for free. But adapting this way of designing is not a trivial task. Despite that, it might be the way to unlock 3D printing as a feasible production method within the construction industry.

Figure 1: Feasible 3D printed solutions might be unlocked through complex, holistic design, which in turn is now possible because of 3D printing

Yet even the widely held belief that complexity comes for free is no longer a widely accepted claim (Kim et al., 2022; Pradel et al., 2017). The consequences of this realization are reflected in the stagnant growth of the 3D printing sector, as pointed out by Peels (2023) in his article, *RIP 3D Printing: 1987–2023, Complexity is Expensive* (Peels, 2023). He does, however, offer a tangible solution, which might provide the way forward for 3D printing.

> "In essence, weve been constructing tools and solutions for a theoretical future rather than addressing the industrys immediate needs. This gap signals unexplored opportunities, offering a glimmer of hope for innovation and growth."

With this in mind, this thesis aims to serve as a case study to approach product design holistically, reasoning from the advantages that come with 3D printing and aiming to meet immediate needs in the built environment.

Section 2

Methodology

To do so, this thesis will offer a thorough evaluation of the strengths and weaknesses of additive manufacturing within the built environment. It will explore what AM in its current form can immediately achieve if it were to be adopted on a large scale within the construction sector and will explore how these factors determine the design requirements for mass-producible 3D-printed solutions. To do so, this thesis is built up out of three distinct parts. The first part explores the impact 3D printing could have on the built environment by first defining concrete goals for the built environment, which will allow the identification of immediate needs within the sector. Secondly, it will explore how the inherent strengths of AM might be optimally exploited to contribute to reaching these goals, and what criteria a design has to adhere to for it to be feasibly 3D printed. Lastly, it will provide an overview of existing research in the field of AM that meets these criteria. Based on this, the following problem statement (PS) has been formulated.

> [PS] Despite decades of development, the adoption of large-scale 3D printing (3DP) in construction remains limited, with a focus on economic gains over innovative design and construction methods, hindering efficiency and radical innovation, while ongoing debate surrounds its cost-effectiveness for traditional building designs, highlighting the need to bridge the gap between theoretical advancements and practical industry needs for innovation and growth within the 3D printing sector.

To research this issue effectively, the following research question (RQ) has been formulated.

> [RQ] How can a shift towards a more holistic design approach facilitate the widespread adoption of additive manufacturing in the built environment, addressing immediate industry needs and fostering innovation and growth?

The research question is further divided into the following sub-questions, which will be answered throughout part one of this thesis. All of them will be answered through literature research.

> [SQ-I] What are the immediate needs in the construction industry?
>
> [SQ-II] How might 3DP contribute to meeting these needs?
>
> [SQ-III] What criteria do 3DP products need to meet to unlock 3DP as a feasible manufacturing method?
>
> [SQ-IV] What existing research exists that meets these requirements?

The second part of this thesis will explore how 3D printing can combine some of the existing concepts into a single, holistic design and create a multi-functional component using a case study. It will also be assessed if the same product can be realized with alternative manufacturing methods, and what the advantages of AM are in comparison, allowing an informed conclusion to be drawn about the added value of 3DP. It will have its own set of sub-questions, which will be formulated based on the findings of part one. This part will also answer the main research question. The third part is reserved for the designing and prototyping of the final product, which will be informed by all the findings of this thesis.

1 PART

3D PRINTING

IN THE BUILT ENVIRONMENT

Section 3

objectives

Given the fact that the built environment is responsible for 30% percent of global emissions according to the International Energy Agency (2022), the most pressing need for the sector is to reach the net-zero emissions (NZE) targets by 2050 (International Energy Agency, 2021, 2022). Currently, however, the sector is far from reaching that goal (International Energy Agency, 2023). To accelerate innovation in the right direction, the IEA has compiled a set of guidelines that they regard as essential to reach the goals (International Energy Agency (IEA), 2022), of which the most relevant for this thesis is the need to renovate nearly 20% of the global existing building stock to zero-carbon-ready by 2030. To reach this objective, an annual deep renovation rate exceeding 2% is required from now until 2030 and beyond. For Europe, this means that 75% of the entire EU building stock which has been identified as low quality will have to be renovated into Near Zero Energy Buildings (NZEB) (European Parliament, 2023). For the Netherlands, this means that 2.5 million dwellings will have to be renovated by 2050 (Volkshuisvesting en Ruimtelijke Ordening, 2022). Achieving the target of retrofitting this amount of buildings to a zero-carbon-ready level by 2030 is ambitious but necessary, and provides a clear and urgent objective for 3DP applications. At the same time, searching for applications in new construction is also relevant, as the IEA estimates a 75% increase in floor area in the next three decades. However, Only 20% of this is expected to be in developed countries. (International Energy Agency, 2022). The challenge faced in Europe is therefore to refurbish. Additionally, solutions that work in renovation will also work in new construction, therefore this thesis will aim to identify applications primarily suited for applications in renovation.

But carbon emissions are not the only concern in the industry. Changing climate and political situations have prompted the World Global Building Council (WGBC) to formulate an additional set of key aspects of sustainable and future-proof design which are (on top of carbon emissions) that the built environment should aim for resilience, circularity, access to water, biodiversity, health, and equity (World Green Building Council, 2023). Even though these are not written specifically to guide innovation, they do provide a clear direction as to where innovation should lead. As such, this thesis will consider carbon reduction, resilience, circularity, health, and equity as the main criteria for innovation in the built environment.

3.1 The potential of AM

Having identified these objectives, it is important to understand what the role of 3DP technologies might be and how they can provide rapid solutions. This has been researched in depth by El-Sayegh et al. (2020). Summarizing their findings, AM holds the potential to increase construction speed, decrease its costs, allow for free-form design, decrease the supply chains, and thus overall increase productivity[1]. On an environmental level, AM makes formwork redundant, generally creates less waste due to its additive (rather than subtractive) nature, and allows the use of recycled materials. The following chapters will explore how these strengths can contribute to reaching the objectives of the built environment formulated in the previous chapter.

1 even though in the history of technology in the context of capitalism, increases in productivity and efficiency have only ever led to people working and consuming more rather than less, meaning that an increase in productivity is only an environmental benefit if the technology is used consciously, as beautifully explained by Hickel in his book *Less is More* (Hickel, 2021)

3.1.1 Carbon

The way 3D printing applications might contribute to carbon reduction is twofold. Firstly, it could result in more energy-efficient production processes. As of present, it is hard to predict the exact impact this will have due to a multitude of uncertain parameters and interactive effects. However, the American Council for an Energy-Efficient Economy (ACEEE) estimates that by 2025 the increased deployment of robots, which 3D printers fall under, will be responsible for 0.57% of the total energy consumption in America (Barnett et al., 2017) and conclude that the overall impact of robots will be a positive one when it comes to reducing carbon emissions, but do stress the importance of keeping track of this number. These gains come from, among others, highly efficient equipment powering robots and the full automation of factories, minimizing lighting and heating requirements, as well as ongoing research and development efforts that focus on enhancing robot efficiency.

On top of that, there are the gains of using recycled materials and the potential to significantly reduce transportation needs. (Ghaffar et al., 2018) (Khajavi et al., 2021). The positive impact AM can have during the manufacturing phase is confirmed by Gebler et al. (2014). In their same research, however, they calculated that an even larger impact, however, will come from the possibilities free-form design has to offer since optimized, lightweight parts will lead to large savings in, for example, the aerospace sector. This shows that the complexity 3DP allows, despite that it does not come for free, holds the potential to result in money and emissions savings elsewhere, which might make the technology feasible overall. However, there are many challenges to be solved before free-form design might lead to such a profound impact due to the complexities it brings with it. (Zhu et al., 2021) (Hinchy, 2019).

3.1.2 Resilience

Another important objective is resilience which, according to the World Green Building Council (2023) comes down to the adaptation of new and existing buildings to new, unpredictable climate situations and the complications that come along with it. This has to be achieved primarily by designing for passive survivability in the event of extended loss of power, heating fuel, or water (World Green Building Council, 2023). In practice, this means that designers should strive for passive solutions for the built environment that do not need electricity or complex systems to function. Castaño-Rosa et al. (2022) researched in depth what this means in practice for the built environment, and found among others that reusing and reimagining existing buildings and materials, following circular construction principles, is crucial to improve the characteristics of (existing) buildings and extending their lifespan. In practice, this might be achieved by implementing passive strategies, including the optimization of a building's orientation to maximize daylight or designing buildings to capitalize on natural ventilation opportunities while ensuring good air tightness, continuous insulation, and high-performance windows to enhance a building's energy efficiency and resilience. What might help to achieve this is the emerging multi-criteria analysis models, which serve as effective tools for assessing the optimal configuration of building components considering context-related characteristics and making sure such solutions result in a building functioning as intended and meeting users' needs. There is no immediate way in which 3DP technologies contribute to this. Rather, these objectives ought to be adopted as guidance during the design process.

3.2 Design for Additive Manfufacturing

Thus far it has been shown that the theoretical benefits of 3DP make the widespread adaptation desirable due to its inherent advantages. Designing solutions to tackle immediate needs will be an important factor in ensuring 3DPs' widespread adaptation. However, it is only part of what might make additive manufacturing feasible. The other part consists of designing for additive manufacturing (DFAM) by understanding the strengths and limitations of the technology.

3.2.1 technical considerations

DFAM is discussed extensively by Gibson et al. (2020) and Hinchy (2019). According to their research, Additive manufacturing should, like any manufacturing method, be considered carefully during the early stages of product design to ensure its suitability and cost-effectiveness, as well as its constraints and common defects, which include (depending on the type of AM) layer heights, support structures, and component orientations. Design features such as overhangs, unsupported elements, small holes, and thin walls must be carefully considered to prevent build failures. Additionally, AM has limitations regarding geometrical tolerances and surface quality, often necessitating post-processing to meet design requirements.

3.2.2 scalability

AM excels in producing complex, customized, low-volume items. However, due to its nature, scaling AM to be a cost-effective manufacturing method is a significant hurdle to be solved before AM will find widespread adaptation. This is because of the slow production speeds, limited material availability, the often required manual post-processing, and the lack of industry-wide standards (Amfg, 2020, October 14). For this reason, other manufacturing methods are often more cost-effective for high-volume, simple products. Since the objective of this paper is to develop a scalable 3D printed product, important factors to consider will thus be the product's function, its performance, complexity, customization, sales volumes, and production times, to understand if it can be feasibly 3D printed on a large scale and to make sure the product exploits the inherent strengths of 3DP.

3.2.3 strengths

To do so, solutions and products should be identified and designed that inherently need to be optimized to meet specific and local needs and requirements, which is also one of the requirements for resilient design. Secondly, since AM is so well suited to handle complexity, this should be exploited by identifying principles that are inherently complex and need to be so to perform their function and create multi-functional and intricate designs that would be challenging or impossible to produce using traditional manufacturing methods to solve complex and multi-faceted problems[2]. Finally, AM supports consolidated manufacturing, where products and components are designed to reduce the need for assembly steps and to streamline the production process. By designing products to capitalize on these strengths, manufacturers can make the most of what AM offers to develop creative and effective solutions (Gibson et al., 2020) and (Hinchy, 2019).

2 This is not the same as deploying AM to enable artificial complexity, serving no other purpose than an aesthetic one at an unreasonable environmental cost, a phenomenon rightfully pointed out by Huston (2024) in his article Architecture and the Environmental Impact of Artificial Complexity.

[I] Mass Customization | Identify products and components that inherently require to be customized.

[II] Inherent Complexity | Identify products and components that are inherently complex (that is, they unconditionally require their complexity to perform) and are near impossible to manufacture with traditional manufacturing methods.

[III] Consolidated Manufacturing | design products and components to be multi-functional and avoid assembly steps.

3.3 applications in built environment

3.3.1 Building envelope

A sensible starting point in the quest to identify complex and multifaceted design problems for 3DP to solve is in the field of building envelopes. Research in this field is plentiful, of which an extensive overview was conducted by Leschok et al. (2023) and Strau (2017). Summarizing their research, they found that current construction practices often result in facades composed of disparate components, each serving distinct and different functions. In contrast, AM holds the potential to integrate various performance aspects into one component, enabling the creation of integrated building components tailored to specific building needs, services, locations, and orientations. considering end-of-life strategies or adopting mono-material designs to achieve sustainability goals. This approach aligns with resilience objectives and opens up opportunities for enhancing indoor air quality, electrical energy production, and reducing energy demand. As a result, 3D printing presents the potential to realize context-specific, high-performance facades. Additionally, the sustainability benefits of material efficiency, reduced waste, and the availability of low-embodied-energy materials are additional possible advantaged of 3D-printed facades as a solution for future building envelope design. Leschok et al. (2023) Did however conclude that such efficient and multifunctional facades are most effective with solutions printed with thermoplastics, while printing with concrete and clay poses more obstacles to achieving holistic design solutions.

Figure 2: 3D printed ventilation channels optimized for efficient air transportation (Schork et al., 2021).

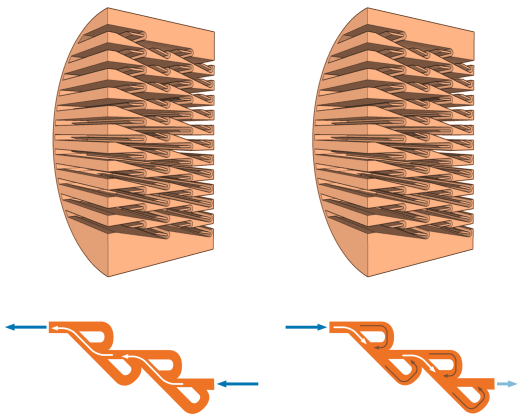

Figure 3: 3D printed FDP to passively regulate air flows in ventilation applications making use of the concept of Tesla valves (Cao et al., 2020)

3.3.2 ventilation

Another area within architecture that poses such multifaceted problems as with facades is ventilation and in particular natural ventilation. This is however one of the strategies identified to be resilient. Natural ventilation relies on air going through openings in the facade, which could be unintentional leakage, inlets, or operable windows. The air is driven inside by natural pressure differences caused by wind and buoyancy (Cauberg, 2005). But ventilating a building in this way has several drawbacks, oftentimes not meeting required ventilation standards due to its reliance on unpredictable weather conditions. Furthermore, the fact that air enters and leaves a building without preheating and heat recapturing makes ventilating this way lead to poor energy performance of a building. This also causes cold drafts, which lead to discomfort and outdoor air pollutants as well as noise coming in (NEN, 2013). Many of these problems were solved by the introduction of mechanical ventilation, but this is expensive, depends on complex mechanical systems, and is therefore not resilient. Despite that, interesting 3D-printed innovations allow more efficient integration of mechanical ventilation in renovation projects, such as highly efficient heat recovery systems (TCPoly, 2021) and optimized ventilation ducting (Schork et al., 2021).

In the case of natural ventilation, however, There are no 3D-

printed solutions that solve all these issues simultaneously. One research by Cao et al. (2020) proposes a 3D printed regulator (which they call Fluid Diode Plate, or FDP in short) of the inflow to solve the issue of poor energy performance. They do this by using Tesla valves, a geometric principle invented by Nikola Tesla in 1920, initially as an unidirectional conduit (diode) for fluids[3]. Its geometry means it does not need any moving parts to control the flow, making it particularly resilient.

3.4 Passive regulation

By exploring these fields of research, it has become clear that above all, passive regulation, be it of air, light, energy flows, or water is a relevant topic. And especially the challenge of combining multiple regulating concepts in one product efficiently. To do so, an overview is required of existing research into such passive, regulating solutions. To further explore this topic, other fields of research where such passive principles have been successfully integrated into 3D printed solutions.

3.4.1 Accoustics

Sound insulation through 3DP can be achieved primarily by making use of the concept of absorption and interference by designing Quarter-wavelength tubes, or quarter-wavelength resonators (QW resonators). These are made up of a tube or cavity which is closed on one end. When the length of the cavity matches an odd multiple of a quarter of the length of an incoming sound wave, it resonates, leading to maximum absorption of sound at these frequencies. The resonators length dictates the primary frequencies at which sound absorption is most effective (Cambonie et al., 2018). One important problem that 3DP has helped solve successfully is that they have to be of rather large lengths to be able to absorb low frequencies (around 68cm for 125Hz and 34cm for 250Hz), which in practice makes them rather difficult to implement (Cambonie et al., 2018). However, they, as well as others, have developed design methods to significantly shorten the required lengths. Cambonie et al. (2018) used origami-based structures to create effective compact QR resonators. Catapane et al., 2023 achieved the same by creating them as spirals, and Setaki (2012) did so by bending them. The last two successfully used AM to realize their designs.

3.5 Case study

To identify a functional case study touching on all aspects of AM that have thus far been described, a multi-faceted problem will be selected for further research. both facade design and ventilation (and in particular natural ventilation), have been identified to be so. A lot of research has already been done into 3D printed, holistic, facade design. This is less true for the problems posed by natural ventilation, even if for all issues it brings (acoustic problems, filtering, and inflow regulation) 3D-printed solutions have been identified. Therefore this thesis will focus on 3D printing in the context of natural ventilation and attempt to bring these existing solutions together into one, holistic design. Particular focus will be put on the concept of FDPs (as proposed by Cao et al. (2020)), as this is one of the lesser researched products.

3 meaning it allows fluids to flow in one direction but stops them from going the other way (Purwidyantri & Prabowo, 2023). Its application has been studied in numerous applications such as heat transfer, fluid mixing, microfluidic control, and gas decompression (Cao et al., 2020) but its application in the built environment has not received much attention yet.

3.6 Conclusion

This part attempted to answer the sub-questions I to IV. The immediate needs in the building sector were identified to be carbon-reducing products and manufacturing techniques capable of making the built environment more resilient and enabling circularity, improving health, and equity. In particular, simple and scalable solutions are required to speed up refurbishment efforts (at least in the EU) [SQ-I]. The inherent qualities of 3DP have shown the technology to be able to do so. Accelerating its widespread adaptation is therefore relevant and desirable [SQ-II]. But for 3DP to become widely adopted, a set of design rules ought to be followed, which are the explicit need for customization, designed to be multi-functional to eliminate assembly steps, and are nearly impossible to manufacture with traditional methods. The resulting products should solve some immediate needs in the industry [SQ-III]. Existing research that complied with these requirements was identified to be in 3D printed holistically designed facades, but also acoustic dampeners, air filters, and regulators (FDPs), especially when these can be integrated into one holistic solution [SQ-IV]. Natural ventilation was identified as a promising case study for the design, as it fits in both with the objective of resilience in the built environment, as well as in the objective to contribute to the refurbishment challenge Europe is currently facing. It is also a complex and multi-faceted problem, which should allow for the design of a multi-functional product that exploits the inherent strengths of 3DP. This will be researched in the second part of this thesis.

PART 2

NATURAL VENTILATION

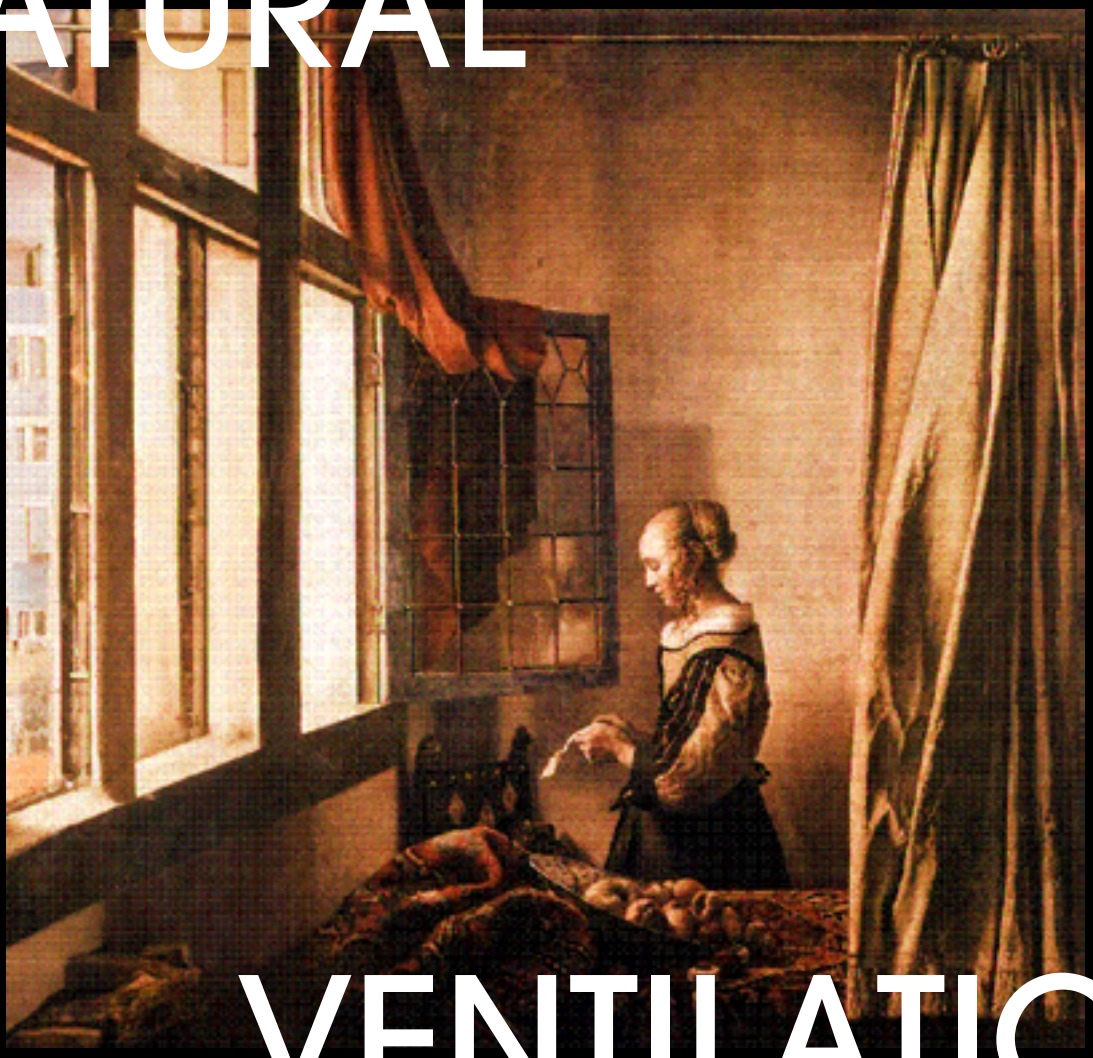

Section 4

Methodology

In the second part of this thesis, natural ventilation, and in particular the FDP, will be researched in depth, to serve as a case study as to how optimizing product design for 3DP might be achieved. For this purpose, the following sub-questions have been formulated, which will be answered throughout this part. Contrary to the first part, this part will be approached mostly by research through design, rather than literature research.

[SQ-V] What is natural ventilation?

[SQ-VI] What makes NV a suitable case for 3DP?

[SQ-VII] What current solutions exist and how might they be improved through 3DP?

[SQ-VIII] How might a solution be optimized for its performance and for AM?

[SQ-IX] How might multiple functionalities be integrated into the solution?

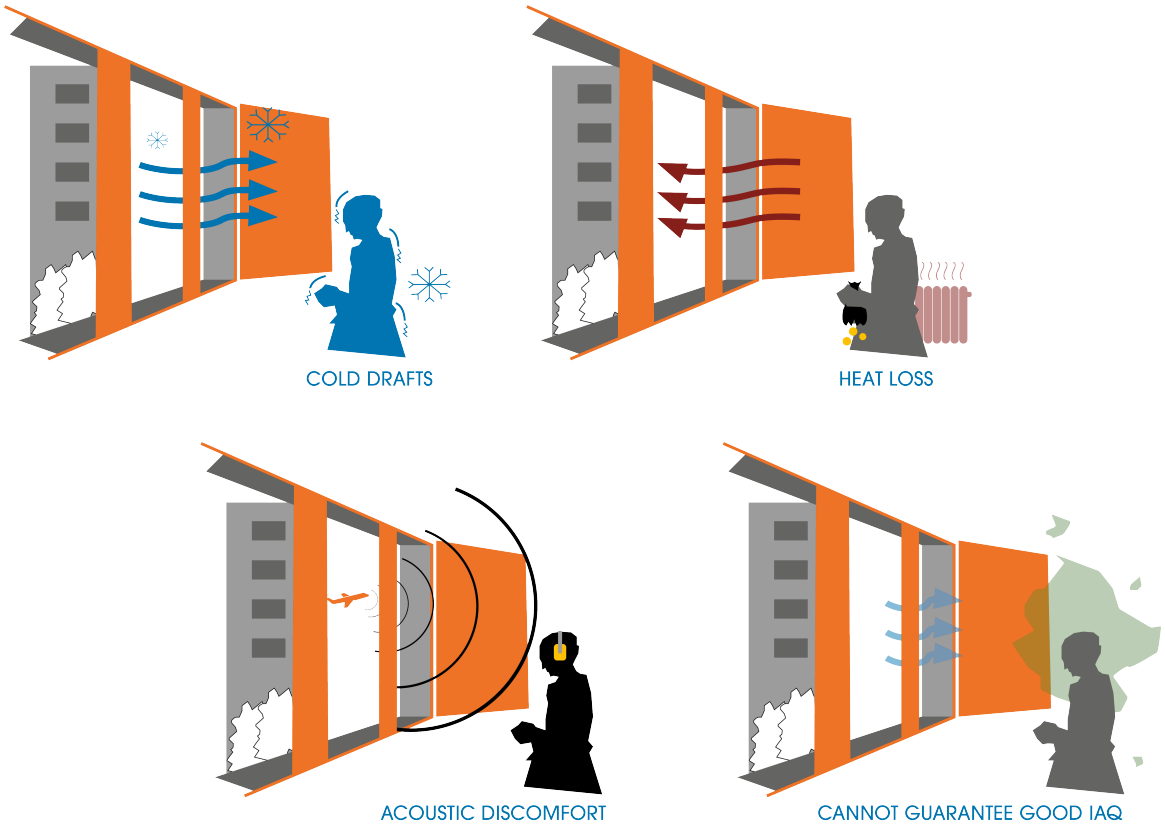

Figure 1: The most pressing issues with natural ventilation (own work)

Section 5

Natural ventilation

Ventilation serves multiple purposes. First and foremost it ensures a healthy indoor climate by providing oxygen, removing indoor pollutants, and regulating indoor humidity. On top of that, it plays an important role in thermal regulation (Biler et al., 2018). Historically, ventilation occurred naturally, driven by natural pressure differences in and around buildings. These are caused by wind and buoyancy, which make fresh air infiltrate through unintentional leaks in the walls (Cauberg, 2005). Still today, in European countries, most of the building stock relies on these natural ventilation principles (Federation of European HVAC associations [REHVA], 2012). But, as discussed in part one, NV has several drawbacks, oftentimes not meeting required ventilation standards due to its reliance on unpredictable weather conditions, its poor energy efficiency, cold drafts leading to discomfort and outdoor air pollutants as well as noise coming in through the openings in the walls(NEN, 2013).

There is however an even more pressing issue, which is the fact that the increasingly strict performance regulations, discussed in Chapter X, for building envelopes pose a problem to NV. This is because the infiltration of air it relies upon is no longer possible through the new, highly airtight facades. If this is not resolved properly, renovated facades result in decreased natural ventilation, with a significant decrease in indoor air quality (IAQ) as a result (Mikola et al., 2022). To avoid this, in modern construction and renovation, pressure differences are mechanically induced (or assisted) by ventilators, ensuring sufficient airflow, while intentional air inlets, called trickle ventilators, or more generally, background ventilators (BVs), are integrated into the windows or walls. These inlets resolve the issue of insufficient ventilation rates but reintroduce the issue of thermal and acoustic discomfort.

5.1 Types of ventilation

To understand different approaches to solving these issues, a better understanding is required of the mechanisms of different types of ventilation strategies. The Dutch building decree (NEN, 2013) distinguishes between four forms of ventilation: type A,B,C and D. Broadly speaking, they can be classified under three ventilation strategies.

Type	Strategy
A	Natural ventilation
B, C	Mechanically driven natural ventilation
D	mechanical ventilation

Table 1: Ventilation stratagies

Type A ventilation relies solely on differences in air pressure in (and around) the building to drive fresh (outside) air inside through unintentional leakage in the construction, operable windows or background ventilators. The main drivers of these pressure differences are wind and buoyancy caused by temperature differences throughout the building. In the case of type B and C, ventilators mechanically create pressure differences in the building. Infiltration is achieved in the same ways as with type A. Since types A, B and C function on very similar principles, they are oftentimes all referred to as natural ventilation. This is also the case in the context of this paper. However, it is important to note that for type A, the regulations are different of that of type B and C,

and will be discussed in chapter 5.1.1 and 5.1.2. Conversely, Type D ventilation regulates the entire ventilation process mechanically.

The use of type A is limited in modern construction (at least in the Netherlands). This is, apart from the aforementioned issues inherent to NV, largely due to the space constraints and stringent design standards for the exhaust ducts (NEN, 2013). Instead, types C and D are the predominant ventilation strategy in modern construction for residences in the Netherlands. All systems have strengths and weaknesses, which will be looked at in more depth in the following chapters.

NV has to occur even at very low pressure differences. In practice, this means its functional components (the background ventilators and other channels) are designed to function with a mere pressure difference of one Pascal, and a wind speed of one meter per second (NEN, 2013). Yet average WS in the Netherlands ranges from 3 to 7 m/s, and speeds of 10m/s are not uncommon. Such circumstances, If there are no measures installed in the BVs, lead to excessive ventilation. This might lead to thermal discomfort, which can be especially uncomfortable if the cold outside air is not mixed well with warm indoor air. Additionally, all this excess fresh air needs to be heated, which significantly contributes to the buildings energy demand, especially during the heating season. . when it comes to noise, BVs in the facade can lead to acoustic discomfort, particularly in urban areas.

Regulation	acceptable range
Minimal functional pressure	1 Pa
Maximal speed in inlet	0.2 m/s

Table 2: Regulations for type A ventilation

Type A ventilations sole dependency on weather-related pressure differences is both its weakness and its strength. It requires no electricity to function and does not require much maintenance, as no ducting and machinery are needed. This makes it by far the most resilient way to ventilate. Additionally, it operates silently. However, its persistent issues in acoustic and thermal comfort are difficult to solve.

5.1.1 Characteristics of type A ventilation

For example, operable windows are a common method to allow for natural ventilation to occur. But open windows expose users to noise, and extended exposure to noise, a problem especially in urban environments, can lead to significant physiological and psychological symptoms, even at low levels (Tang, 2017). This has the undesired effect of users having to choose between good air quality, acoustic comfort, and thermal comfort. A lack of either three of them can have (serious) health implications. Designing mutually exclusive ventilation, thermal, and noise solutions, is therefore not sufficient to achieve a healthy indoor environment. Instead, a more holistic approach to natural ventilation is required, taking into account efficiency, health, and resilience. The importance of solving them can not be overstated, since both insufficient ventilation as well as acoustic and thermal discomfort can have serious health consequences, summarized by the Healthy Buildings Program (2017).

Yet mutually exclusive design measures remain persistent, as shown by a study by the Acoustics & Noise Consultants (2020), who assessed 122 planning applications in the UK. For 85% of them, preventing overheating relied on open windows, while achieving acceptable noise conditions relied on having the windows closed. As such, it becomes clear that marrying natural ventilation, noise mitigation and thermal comfort together into a sufficient and holis-

tic climate-responsive design can prove difficult, as often each aspect of this trinity requires conflicting measures.

5.1.2 Characteristics of type C ventilation

Type C ventilation shares many characteristics with type A. Its additional benefits come from the fact that mechanical ventilation makes it a more reliable system, which is less dependent on the weather. Yet here too, without measures, weather can influence its performance negatively, since it still relies on openings in the facade. Too much wind will have the same negative effects as with type A.

In case of type C strategies, cross ventilation can happen as well, but is in its entirety undesired, as the additional airflows are not needed to reach the required minimal ventilation (as is sometimes the case with type A), but does cause undesired heat loss. This too has to be accounted for in the design of the BVs.

Thermal and acoustic concerns are the same as with type A, but with the ventilators as an additional source of noise.

When working with type C ventilation, a pressure difference of 5 Pa can be assumed (Nijeboer & Hage, n.d.)

Regulation	acceptable range
Minimal functional pressure	5 Pa
Maximal speed in inlet	0.2 m/s

Table 3: Regulations for type C ventilation

5.1.3 Characteristics of type D ventilation

With type D ventilation, in contrast to NV, air is mechanically led into the building, after which it gets heated up and filtered before properly entering the building's interior through extensive duct systems. Air removal happens mechanically as well, which allows heat to be recaptured by a heat exchanger, as to minimize energy loss due to ventilation. A significant advantage of MV is that no direct openings in the facade are necessary to facilitate its processes, thus acoustic problems are mitigated completely. The energy needed for this process gets (more than) compensated by the heat recapturing.

It is for these reasons that new constructions often deploy type D ventilation, which solves all these issues. However, due to its complexity and reliance on ducts, MV is expensive to install. In practice, this leads to its application mostly in wealthy countries (there is a clear correlation between the scale of application of MV and the wealth of a country, according to the Federation of European HVAC associations [REHVA] (2012). Additionally, it is particularly difficult to fit MV into renovation projects. Therefore, it is most suitable for new construction projects.

Type	Ventilation efficiency	Acoustics	Thermal comfort
A	-	-+	-+
B	-+	-+	-+
C	-+	-+	-+
D	+	+	+

Table 4: Ventilation stratagies

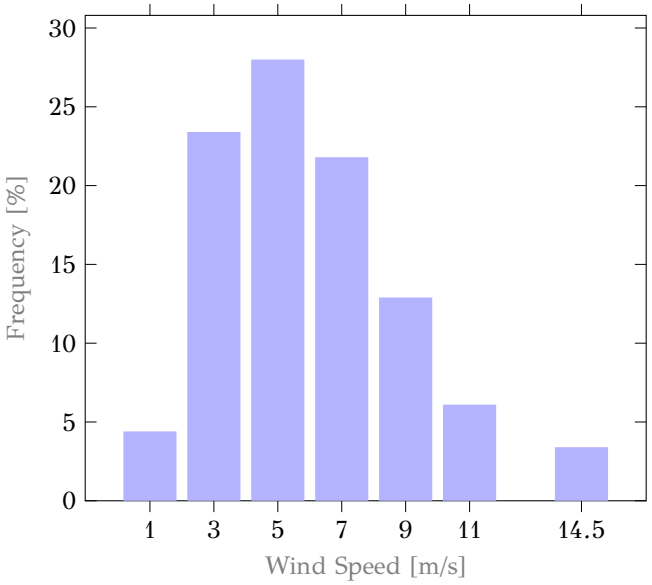

Figure 2: Wind speed frequencies in the Netherlands (Cauberg, 2013)

5.2 3DP and NV

Since this thesis set out to focus primarily on renovation applications, it will henceforth focus on types A and C. Many of the issues with these two strategies come from the fact that rely on background ventilators. The apparent objective therefore becomes to research how background ventilators might be improved upon through 3D printed solutions. But to do that, a better understanding of the functions of trickle ventilators and background ventilators is required.

5.3 Background ventilators

A holistically designed background ventilator should have a sufficient ventilation capacity, offer control over the inflow, provide thermal and sound insulation, and ideally filter pollutants. Additionally, it should be water resistant, offer some security features, and be adaptable to various climates (Biler et al., 2018) (Daniël, 2021). The next chapters will evaluate the existing solutions for the most important of these aspects.

5.3.1 Inflow regulation

The most basic type of BVs are manually adjustable ones. They allow the user to adjust the amount of air entering into the room. As such, when wind speeds are high, or when there is excessive noise outside, their negative effects can be manually regulated, based on preferences. This solution is however still a compromise between sufficient ventilation, thermal & acoustic comfort. More importantly, users often forget to reopen the BVs after the hindrance is over, meaning long periods of minimal ventilation can occur. Unwanted cross ventilation can not be prevented by these types of opening, unless they are closed.

In order to avoid inefficient ventilation caused by users, there are self-regulating systems on the market, which broadly fall in two categories: wind-pressure regulated or electrically regulated. The former closes mechanically based on wind-pressure sensitive parts. They are sufficient in preventing excessive ventilation with high wind pressure (they typically react when pressures reach 5 - 10 Pa), but since they are not sensitive to changes of wind pressure in the low range (0 - 5 Pa), they still do not solve all issues. NV systems are designed to already function properly at a wind pressure of 1 Pa, so with a slight increase there might already be an unpleasant draft, and cross ventilation might still take place. The latter solves nearly all these issues. It regulates the BV electronically, based on an pressure sensor. This means that even at low pressure differences (0 - 5 Pa) the system can adapt. These sensors even react to cross ventilation, and are able to counter it effectively by closing.

All these solutions offer their advantages, but it should be noted that none of them are passive, which is an important objective for this research.

5.3.2 Insulation

To provide acoustic insulation, all versions can be fitted with acoustic lining, which absorbs sounds passively. This is a very effective solution. However, there is a large difference in their ability to insulate high and low frequencies. This is because for porous or fibrous insulating materials to absorb lower wavelengths, they would require a thickness in the same order of magnitude of the sound waves (Berardi & Iannace, 2015), which can be very large in lower frequencies. Yet it is in the low frequencies in particular where traffic and vehicle-induced noise carry a lot of energy and

induce a significant discomfort for humans (Can et al., 2010), and therefore poses an important issue to solve.

For this reason, QW resonators offer an interesting solution, as they have been shown to possess excellent capabilities to absorb lower-frequency sound waves. Arjunan (2019), for example, reached near-perfect sound absorption on the lower side of the spectrum (475Hz).

Incorporating them in a BV has been trialed in research conducted by (Field, 2004) . He obtained a weighted sound reduction index of his proposed device of around 22 dB. However, in a critical comparison between noise mitigating solutions in naturally ventilated buildings, Tang (2017) states the proposed ventilator occupies a large area while the ventilator opening size is small, which is not beneficial for NV, which needs larger openings to function with the small pressure differences that drive it (De Salis et al., 2002). However, 3DP has been proven to be able to make QW resonators much more compact (Cambonie et al., 2018; Catapane et al., 2023; Setaki et al., 2023), which have theoretically made it possible to implement this concept in background ventilators whilst taking up significantly less space than the concept of Field (2004).

Additionally, the amount of sound absorption also depends on the length of the inlet, where longer channels absorb more sound (De Salis et al., 2002). This is the reason why in case of heavy noise pollution, even if generally installing BVs in windows is preferred to their wall-integrated counterparts since require a significant diameter to provide the same airflow, a wall inlet is preferred, due to their increased sound insulation (Eco traject, 2016).

According to De Salis et al. (2002), optimal performance when it comes to sound insulation might come from combining multiple concepts. A hybrid solution could exploit the strengths of lined inlet ducts (good airflow and absorption in high wavelengths).

Despite their use of insulating materials, none of the background ventilators provide thermal insulation (Daniël, 2021).

5.3.3 Filtering

In contrast to MV, which by default uses HEPA filters to remove pollutants, air filtering is much more challenging to combine with NV. Especially since filters tend to increase the air resistance, and therefore reduce the capacity of background ventilators. Generally, the measures installed are limited to coarse grills, aimed primarily at keeping out animals and other objects.

5.4 Duco Silenzio

An example of a background ventilator that already solves most issues well is the Duco Silenzio (Duco, 2024a), which is shown in figure 3. However, to achieve its high performance, it relies on many separate parts and relatively complex, mechanical solutions, making it an expensive product (prices range from 400 to 650 euros, based on the provider, reducing their applicability in less wealthy countries) maintenance-heavy, and more prone to failure. The goal of designing a 3D-printed background ventilator would therefore be to achieve similar performance for a lower price. But implementing a passive, yet effective solution requires a holistic approach to these problems, both to solve the inherent problems of NV, but more importantly, to allow 3DP, expensive as it is, to be a feasible means of production. Unlocking the potential power of 3DP in the context of NV will therefore be the main objective of this paper.

The most important issue to solve is the inflow regulation, since as of yet there is no passive manner to do so. Manual systems

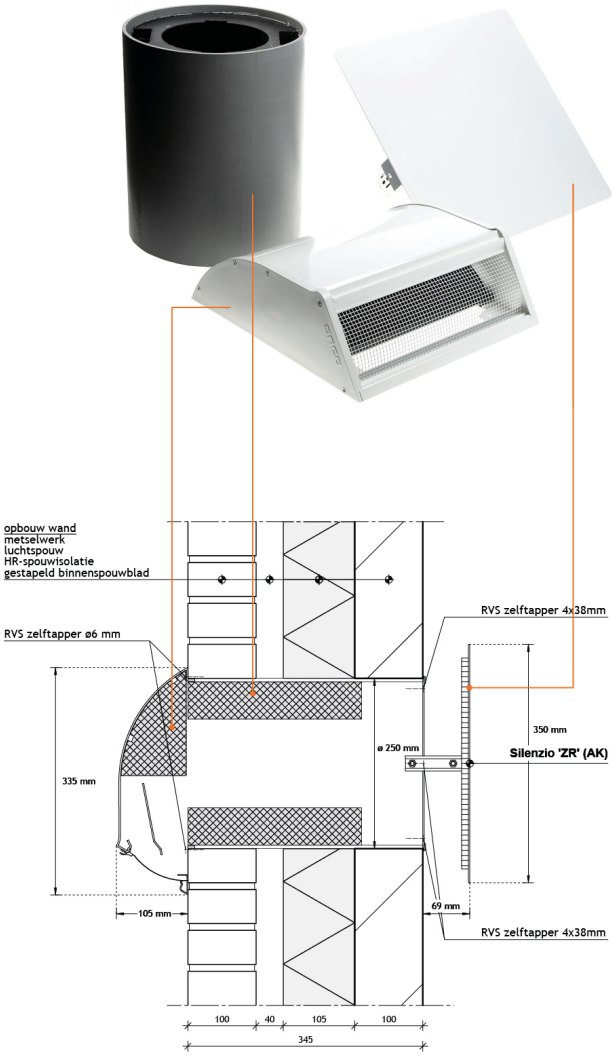

Figure 3: The Duco Silenzio solves most issues that NV poses, but does so with relatively high complexity and at a relatively high cost (Duco, 2024a)

lead to improper usage, and self-regulating systems are complex. Therefore, this will be the main focus of this thesis. Additionally, the acoustic and filtering solutions from Part 1 will included. Additionally, explore if filtering measures can be implemented, which would add new functionality to the BV which it currently does not possess.

5.5 Conclusion

This chapter explored what natural ventilation entails [SQ-V] and how its complex and contradictory requirements might be solved through 3DP by utilizing (improvements of) passive principles such as FDPs, QW resonators, and cyclone separators [SQ-VI]. Many of the complexities have been resolved by background ventilators, however, in their current state, they are successful in doing so only to a certain extent. Additionally, the systems that solve the problems of NV most effectively are those that rely most on separate, electronic, and moving parts. Therefore, there is a large potential for 3DP to provide a passive and holistic solution [SQ-VII]. The next chapters will focus on the question if these mechanical solutions can be replaced by 3DP-enabled, passive geometrical solutions while reaching the same levels of performance, primarily when it comes to inflow regulation through the use of FDPs, but also when it comes to acoustic insulation and air filtering, attempting to answer the remaining sub-questions [SQ-VIII and SQ-IX].

Although Type A regulations are the most stringent and least commonly used, designing to meet these standards ensures compliance with the more commonly applied Type C regulations, thus aiming to meet the requirements for Type A during the design process will ensure its broader application, also in combination with Type A.

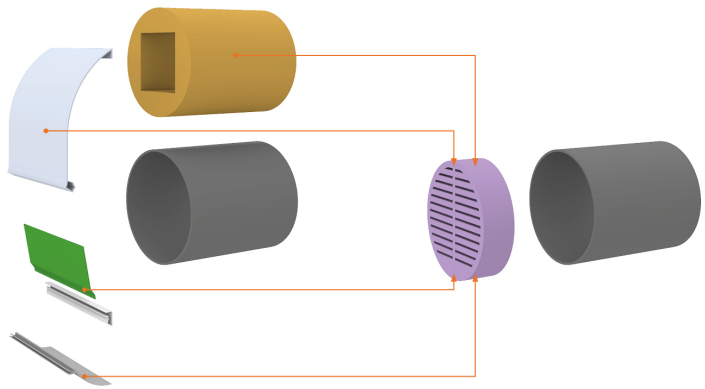

Figure 2: The objective during the design process will be to try and integrate all functionalities of a standard BV into one, multi-functional component

Section 6

FDP

This chapter will research the concept of FDPs. To do so, this chapter will propose a numerical method to approach the behavior of FDPs and compare their performance to the norms as prescribed by the Dutch building regulations. Then, the fabrication methods are explored, and the performance of a physical model is tested against the numerical model. Lastly, a holistic integration of FDPs into background ventilators is explored.

6.1 Previous research

The concept of the Fluid Diode Plate (FDP) was introduced by Cao et al. (2020). Their research aimed to optimize and use the diode-like characteristics of Tesla valves by efficiently integrating them into an infinitely expandable, passive check valve (which they refer to as an FDP) to prevent back-flow in large ventilation channels. However, the concept of FDP also lends itself to regulating inflow in natural ventilation applications. This application was researched by Hu et al. (2024), who continued the research of Cao et al. (2020). and optimized the Tesla valve for this specific application.

In their paper in which Cao et al. (2020) first introduced the concept of the FDP, they started by 3D printing one and testing its performance in a wind tunnel. They then proceeded to use this data to verify their subsequent simulations. To find an optimized Tesla valve, they simulated 21 iterations of valves, varying the number of flow loops and channel ratios, as well as the porosity (the amount of open area of the FDP that air can flow through) of the FDPs. They found that with increasing wind speeds, the pressure drop in the backward direction indeed increased significantly, while in the forward direction, it remained close to a pressure drop over a grille with similar porosity.

Varying the number of flow loops, N, they found that with not more than two of them, there was little difference in the pressure drop between the backward and the forward direction. With a larger number of flow loops, however, the pressure drop in the backward directions increased significantly, while remaining low in the forward direction. They also concluded that the channel ratio, η (the ratio between the height of the main channel, H, and that of the side channel, h) influences the performance of the FDP, with increased performance with higher channel ratios (Cao et al. (2020) identified $\eta = 0.63$ to be the most efficient within their set of simulations). Similarly, they found the effect of the porosity of the FDP to influence its performance strongly. FDPs with the same channel ratio but lower porosities offer more resistance in the backward direction due to increased turbulence in the channels. However, decreasing the porosity while maintaining a high η means a significant increase in the thickness of the FDP. Their simulations lead to a maximal diodicity of 6.

Continuing on this research, Hu et al. (2024) researched in more detail the effect of the slope angles and channel dimensions on the valve's effectiveness. By doing so, they significantly improved the performance of the Tesla valve as proposed by Cao et al, reaching a diodicity of 22. In order to find the optimum, Hu et al. (2024)the values of L, H_2, H_3 and θ and quantifying the influence of the dimension of each parameter on the effectiveness of the valve. They concluded that for L, a length lower than 25 mm resulted in an increased pressure loss in the backward flow direction. Lengths higher than 25 mm resulted in a reduced pressure drop (and therefore less regulation capabilities). For H_2, they

found that values between 1.75 mm and 2.00 mm resulted in an increased pressure drop, whereas widths over 2.00 mm resulted in no further improvement. Furthermore, they concluded that the smaller the value of H3 (that is, the thinner the baffle), the bigger the resulting pressure drop, and is therefore mostly dictated by the limitations and precision of the manufacturing method. The effect of varying θ was relatively small, showing the best performance around 230°. The results have been summarized in table 5.

Parameter	Ideal range
L	$<$ 45 mm
$H2$	1.75 mm – 2.00 mm
$H3$	$<$ 1 mm
θ	210° - 230°

Table 5: Optimal values for each parameter of the Tesla valve (Hu et al., 2024)

From the 16 variants, the best-performing was selected to be further simulated and compared to the best-performing valve that came out of the research of Cao et al. Both sets of parameters are included in table 6. These parameters will be used throughout the rest of this paper, as they result in the best-performing Tesla valve. However, it is important to note that there are further optimizations possible. This valve was selected as it performed best out of all simulations, but further research might reveal even better-performing valves. Furthermore, other research has shown that valves with differently shaped side channels or topology-optimized valves can perform even better, which will be expanded upon in chapter 11. There are however restrictions to these optimizations, as not all geometries can be effectively fitted into FDPs, as will be explained in the next chapter.

Group	$H1$	$H2$	$H3$	L	θ
(Cao et al., 2020)	5 mm	3.58 mm	1 mm	15 mm	210°
(Hu et al., 2024)	5 mm	2.66 mm	1.61 mm	26.8 mm	195°

Table 6: The valve parameters found to cause highest pressure loss (Cao et al., 2020; Hu et al., 2024)

6.2 FDP design

Since FDPs consist of many stacked valves, An important limiting factor for their optimization is the need to stack the valves compactly to maximize the control over the porosity of the FDP, which in turn strongly influences its performance. Furthermore, the valves must lend themselves to be extruded and adapted in a variety of shapes for them to be widely applicable, as this adaptability is one of the strengths of FDPs over conventional regulatory systems.

The objective of flexibility also complicates the practicalities around the FDP. In particular, since ventilation requirements vary significantly per building, each FDP will have to be optimized to function optimally in their particular application. Since performing CFD analysis is time-consuming, Cao et al. state that for FDPs to find widespread adaptation, a method to determine the appropriate FDP specification for any application has to be developed, which can also take into account parameters such as inflow direction, which are important factors in ventilation engineering. A

proposal of what such a model might look like is given in chapter 7

Additionally, measures should be taken to prevent internal deposits, while other geometric and material choices could improve its acoustic performance. All of this should however integrated without jeopardizing the efficiency and customization of the FDP, A trade-off which will be explored in depth in chapter 12.

6.3 Performance indicators

The objective when designing the Tesla valve for integration into FDPs is to optimize its ability to regulate inflow, which is achieved when the pressure drop over the FDP in the reverse direction is as high as possible, particularly at high winds speeds. Additionally, maintaining a pressure drop in the forward direction that is as low as possible can be beneficial for other applications of FDPs, but when it comes to regulating inflow, this is of lesser importance. The ratio of the pressure drop in the forward and backward direction is commonly referred to as diodicity, Di.

$$\Delta P_R = P_1 - P_2 \tag{1}$$

$$\Delta P_F = P_2 - P_1 \tag{2}$$

$$Di = \frac{\Delta P_R}{\Delta P_F} \tag{3}$$

P = Air pressure [Pa]

The reason why the Tesla valves show this diodic behavior is that when a fluid moves through the valve (which is generally made up of a main channel, a bypass channel, and a baffle separating them both) in the forward direction, it mostly stays in the main channel, with little flow in the bypass channel. However, in the reverse direction, the fluid enters the bypass channels. This creates collision with the fluid that travels through the main channel, causing turbulent flows filling the channel with vortices that disrupt currents, resulting in a pressure drop when the flows meet(Peng et al., 2023). As such, it offers minimal resistance to forward flow but significant resistance to reverse flow, especially at higher flow rates. If this pressure drop is larger than the initial pressure driving the fluid, it will cause the fluid to stop entirely (Cao et al., 2020). This behavior is ideal for regulating natural ventilation, as little resistance to the inflow as possible is required at low wind speeds, while large resistance is required at high wind speeds, as discussed in chapter 5.3.1.

6.4 Inlet capacity

The capacity of a background ventilator and the speed with which the air is flowing through it depends on various factors and is determined by the pressure difference over the inlet, which in turn is determined by the inlet's resistance. This resistance is typically represented by its flow coefficient, C_v (van Herpen, 2005).

6.4.1 Flow coefficient

The flow coefficient C_v quantifies the resistance encountered by the airflow within an inlet. It accounts for the collective impact

of minor loss coefficients, ζ, associated with various components within the inlet, such as valves, grilles, and contractions. These coefficients are dimensionless parameters reflecting the efficiency with which these components facilitate fluid flow and the energy loss caused by flow disturbances. The flow coefficient, C_v, can be determined by the formula (van Herpen, 2005):

$$C_v = \frac{A \cdot \sqrt{\frac{2}{\rho}}}{1 + \sqrt{\lambda \cdot l/D_h + \Sigma\zeta_i}} \tag{4}$$

C_v = Flow coefficient [–]
A = Area of the inlet [m^2]
ρ = Density of air [kg/m^3]
λ = Friction factor [–]
l = Length of the flow path [m]
D_h = Hydraulic diameter [m]
$\Sigma\zeta_i$ = Sum of minor loss coefficients (dimensionless)

Essentially, the flow coefficient quantifies how efficiently a valve can pass a fluid through it under a pressure difference of 1 Pascal, with lower values indicating more restrictive flow and higher values indicating less restrictive flow. With standard grilles, C_v is a constant. With Tesla valves, however, C_v decreases as wind speeds increase, meaning that at high wind speeds, it will restrict airflow significantly more than at low speeds, for reasons explained in chapter 6.

6.4.2 Volumetric ventilation rate

The volumetric ventilation rate Q through an inlet is given by the formula (van Herpen, 2005) and can be determined with the background ventilator's C_v :

$$Q = C_v \cdot (\Delta P)^{\frac{1}{n}} \tag{5}$$

Q = Volumetric ventilation rate [m^3/s]
C_v = Flow coefficient $Pa^n m^3/s$
ΔP = Pressure difference [Pa]
n = flow behavior index [–] (typically 1 for laminar flows and 2 for turbulent flows)

Once the capacity of an inlet is determined, the airspeed can easily be obtained with the formula:

$$v_{inlet} = \frac{Q}{A} \tag{6}$$

v_{inlet} = air speed in the inlet [m^3/s]
A = area of the inlet m^2

6.4.3 Hydraulic diameter

As shown in 4, The C_v of a background ventilator depends, among others, on its hydraulic diameter, commonly denoted as D_h, d_h, or simply D. This geometrical property provides a way to simplify calculations for pressure drop and fluid flow rates in non-circular pipes and ducts by treating them as if they were circular (Neutrium, n.d.). The hydraulic diameter can be calculated as follows (Engineeringtoolbox, 2024b):

$$D_h = \frac{4 \cdot A}{P} \tag{7}$$

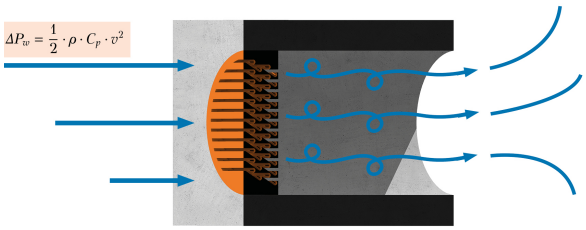

Figure 4: The pressure on a facade can be determined using equation 15

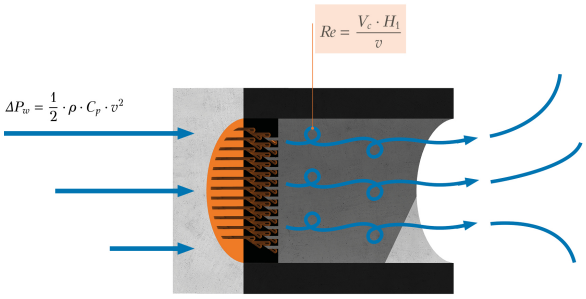

Figure 5: The Reynolds number in the FDP is determined with the equation 12

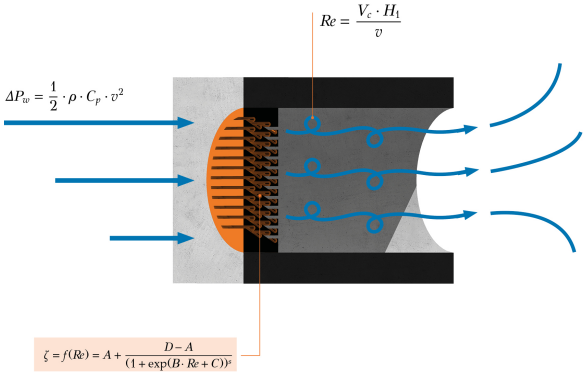

Figure 6: The resistance of the FDP is given by its performance curve, which is given in equation 13, based on the simulations of Hu et al. (2024)

D_h = Hydraulic diameter [m]
A = Area of the valve [m^2]
P = Circumference of the valve [m]

In the case of circular conduits, as is the case with the Tesla Valve, D_h equals the diameter of the conduit.

$$D_h = D \tag{8}$$

D_h = Hydraulic diameter [m]
D = Diameter of the circular valve [m^2]

6.4.4 Porosity

In a standard background ventilator, most of the losses will be caused by the grille. The magnitude of these losses depends largely on the porosity, a, of the grille. This is also true for FDPs, where a part of the resistance of an FDP is caused simply by its low porosity. In the context of grilles and FDPs, porosity refers to the ratio between the free area through which the air can flow and the total area [4].

$$a = \frac{A_{\text{free}}}{A_{\text{total}}} \tag{9}$$

a = Porosity [m^2]
A_{free} = Open area [m^2]
A_{total} = Total area [m^2]

To verify how much additional resistance the internal geometry of the FDP (the Tesla Valves) offers on top of that caused by their porosity, their performance should be tested against that of a standard grill with the same porosity. Some standard values for minor loss coefficients are listed in table 7.

a	ζ
0.7	3
0.6	4
0.5	6
0.4	10
0.3	20
0.2	50

Table 7: Minor loss coefficients for different grille porosities (Engineeringtoolbox, 2024a)

6.4.5 Reynolds number

The reason why porosity influences the minor loss coefficient of a grille is because it directly influences the Reynolds number of the air flows through the grill. The Reynolds number, Re is a dimensionless quantity to characterize (among others) the flow of fluids through openings. Re shows the relative importance of inertial and viscous effects in the flow dynamics.

$$Re = \frac{V_c \cdot D_h}{\upsilon} \tag{10}$$

with

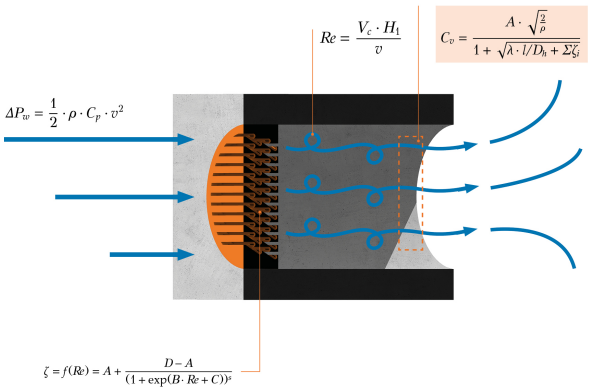

Figure 7: The flow capacity of the inlet is mostly determined by the resistance of the FDP, and can be obtained using equation 4

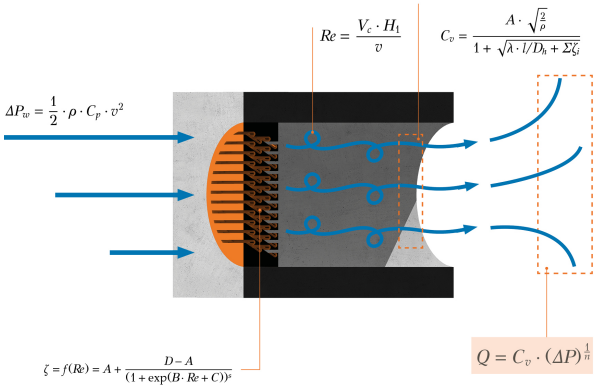

Figure 8: The volumetric ventilation is determined with equation 5

4 When performing simulation on a single Tesla Valve, a equates to 1.

$$V_c = \frac{V}{a} \tag{11}$$

Re = Reynolds number [–]
H_1 = Height of the main channel [m]
v = Kinematic viscosity of air ($1.5 10^{-5}$[m^2/s])
V_c = Average speed in main channel [m/s]
V = Air speed [m/s]
a = Porosity [–]

However, as we have seen in formula 8, in the case of circular valves D_h equals its diameter. Therefore Re is expressed as:

$$Re = \frac{V_c \cdot H_1}{v} \tag{12}$$

When Re is low ($Re < 2300$ for air in a pipe system (Engineeringtoolbox, 2024b)), viscous forces are relatively dominant. leading to laminar flow characterized by smooth, predictable streamlines. On the other hand, at high Reynolds numbers ($Re > 4000$ for air in a pipe system (Engineeringtoolbox, 2024b)), inertial forces predominate, resulting in a turbulent flow marked by chaotic fluctuations and mixing. When passing through an FDP, large Reynolds number will be introduced into the flow due to its low porosity and the structure of the Tesla valves. This effect increases when wind speeds increase (Cao et al., 2020).

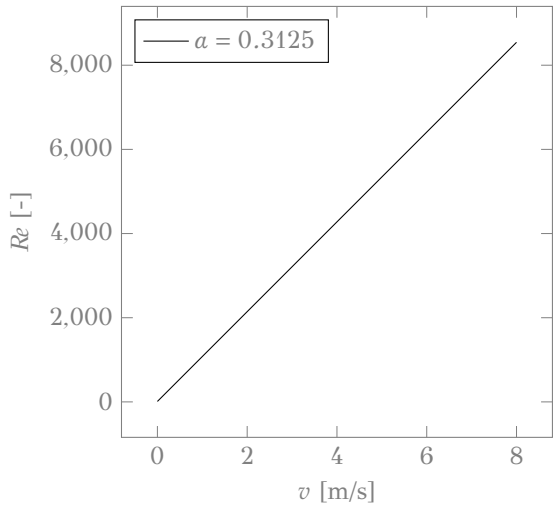

Figure 3: Reynold numbers according to formula 12 with $a = 0.3125$

6.5 Simulation results

To establish the relation between the minor loss coefficients, ζ, and the flow speed through the FDP, Hu et al. performed a second set CFD analyses (figure 4). This time, they simulated two units in a row with the optimized specifications that resulted from their previous CFD studies, listed in table 6. As an FDP is infinitely expandable, they assumed every valve to perform similarly and therefore simulated only one row (made up of the four units).

When plotting the resulting minor loss coefficients of the valve against the Reynolds numbers, they found they could be fitted with a five-parameter logistic function (equation 13).

$$\zeta = f(Re) = A + \frac{D - A}{(1 + \exp(B \cdot Re + C))^s} \tag{13}$$

ζ = Minor loss coefficient [–]
Re = Reynolds number [–]

This curve is referred to as the performance curve of the valve. The appropriate parameters for the performance curve for both their simulations and that of Cao et al. are provided in 6[5] and are plotted in figure 9.

A	B	C	D	s
68.0	-1.93×10^{-3}	0.3999	12.91	0.04654
170.0	-8.46×10^{-3}	6.314	8.17	0.0416

Table 8: Parameters for five-parameter logistic function for Cao et al. (2020) and Hu et al. (2024)

The performance curve allowed Hu et al. to perform a final CFD simulation to obtain the volumetric ventilation rate through an FDP in a practical scenario (figure 10). To do so, they modeled a small, rectangular building with two identical openings (1840x720 mm) on either side. One of the openings was fitted with a surface to which the regulatory behavior of the FDPs was assigned using the performance curve (rather than modeling and simulating a large FDP, running the risk of the complex geometry of the FDP would introduce instability into the simulation). Using reference speeds of 0, 2, 4, 6, and 8 m/s, denoted as U_{ref}, this allowed them to simulate FDPs performance in a realistic scenario. The results of the CFD were translated into a Normalized volumetric ventilation rate, by dividing the volumetric ventilation rate by the area and the air velocity. The results are plotted in figure 10. This dimensionless metric not only shows the increased regulatory capabilities of FDPs at higher wind speeds, but also serves as a reliable way to compare the accuracy of different simulation and calculation methods and will be used as such to test the accuracy of the numerical method of approximating the FDP's performances.

$$Q_n = \frac{Q}{whU_{ref}} \tag{14}$$

Q_n = Normalized volumetric ventilation rate [–]
Q = volumetric ventilation rate [m^3/s]
w = FDP width [m]
h = FDP height [m]
U_{ref} = Reference wind speed [m/s]

But as remarked by Cao et al., performing a CFD analysis for every variation and application of an FDP is time-consuming and complex, and stands in the way of widespread adaptation of CFDs. Therefore, a numerical method will be proposed in chapter 7 using the performance curve as a basis to predict the FDP's performance. The results of this model can be tested against that of the final CFD simulation, by translating the simulated ventilation rates into a normalized volumetric ventilation rate, by dividing it by the area and the air velocities. The results are plotted in the figure 10. This dimensionless metric not only shows the increased regulatory capabilities of FDPs at higher wind speeds, but also serves as a reliable way to compare the accuracy of different simulation and calculation methods and will be used as such to test the accuracy of the numerical method of approximating the FDP's performances.

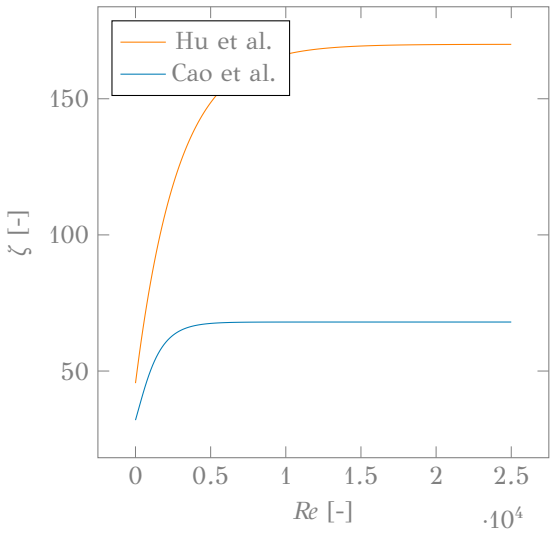

Figure 9: The performance curves for Cao et al. (2020) and Hu et al. (2024)

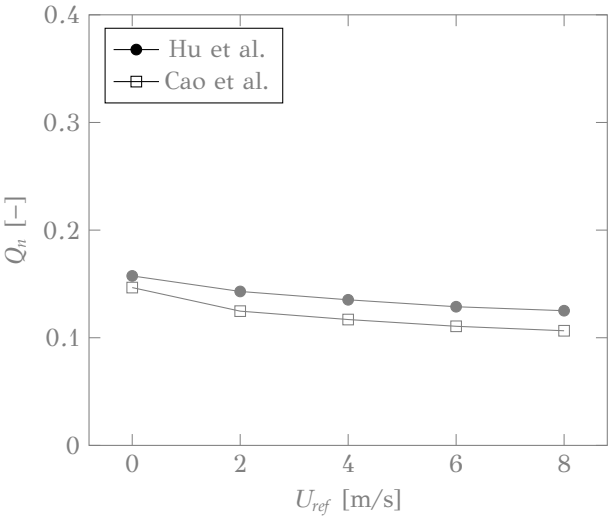

Figure 10: Normalized volumetric ventilation rate

5 These values differ from the original ones in the paper of Hu et al., as the numbers they provide do not match the graph they present. The author of this paper has taken the liberty to change the incorrect parameter values to match the graph plot provided by Hu et al.

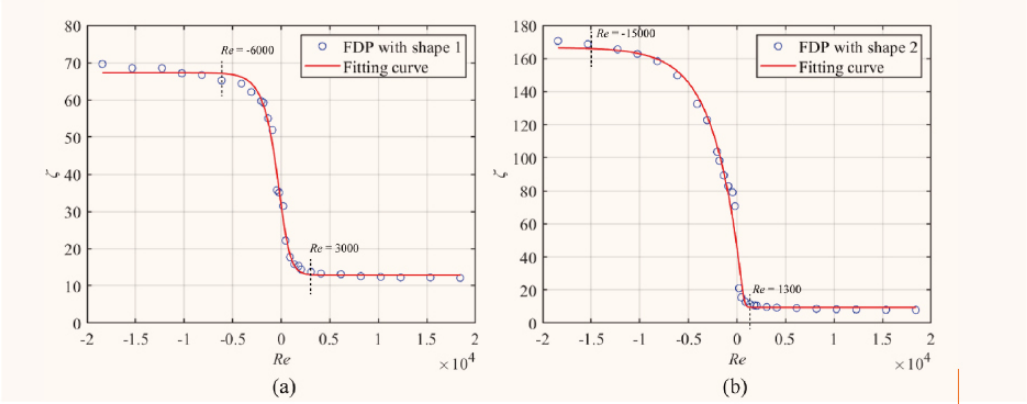

PERFORMANCE CURVES

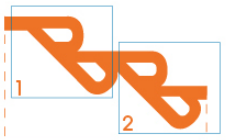

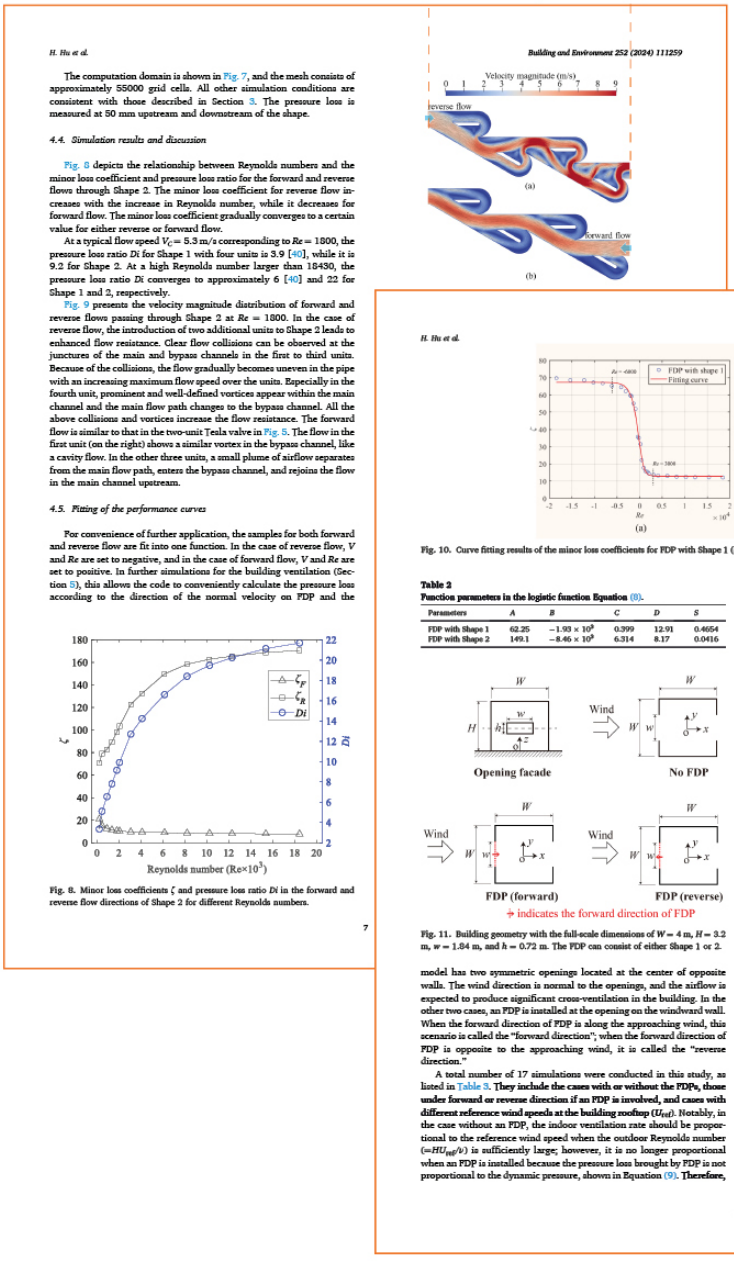

H. Hu et al. Building and Environment 252 (2024) 111259

The computation domain is shown in Fig. 7, and the mesh consists of approximately 55000 grid cells. All other simulation conditions are consistent with those described in Section 3. The pressure loss is measured at 50 mm upstream and downstream of the shape.

4.4. Simulation results and discussion

Fig. 8 depicts the relationship between Reynolds numbers and the minor loss coefficient and pressure loss ratio for the forward and reverse flows through Shape 2. The minor loss coefficient for reverse flow increases with the increase in Reynolds number, while it decreases for forward flow. The minor loss coefficient gradually converges to a certain value for either reverse or forward flow.

At a typical flow speed V_c = 5.3 m/s corresponding to Re = 1800, the pressure loss ratio Di for Shape 1 with four units is 3.9 [40], while it is 9.2 for Shape 2. At a high Reynolds number larger than 18430, the pressure loss ratio Di converges to approximately 6 [40] and 22 for Shape 1 and 2, respectively.

Fig. 9 presents the velocity magnitude distribution of forward and reverse flows passing through Shape 2 at Re = 1800. In the case of reverse flow, the introduction of two additional units to Shape 2 leads to enhanced flow resistance. Clear flow collisions can be observed at the junctures of the main and bypass channels in the first to third units. Because of the collisions, the flow gradually becomes uneven in the pipe with an increasing maximum flow speed over the units. Especially in the fourth unit, prominent and well-defined vortices appear within the main channel and the main flow path changes to the bypass channel. All the above collisions and vortices increase the flow resistance. The forward flow is similar to that in the two-unit Tesla valve in Fig. 5. The flow in the first unit (on the right) shows a similar vortex in the bypass channel, like a cavity flow. In the other three units, a small plume of airflow separates from the main flow path, enters the bypass channel, and rejoins the flow in the main channel upstream.

4.5. Fitting of the performance curves

For convenience of further application, the samples for both forward and reverse flow are fit into one function. In the case of reverse flow, V and Re are set to negative, and in the case of forward flow, V and Re are set to positive. In further simulations for the building ventilation (Section 5), this allows the code to conveniently calculate the pressure loss according to the direction of the normal velocity on FDP and the

Fig. 8. Minor loss coefficients ζ and pressure loss ratio Di in the forward and reverse flow directions of Shape 2 for different Reynolds numbers.

7

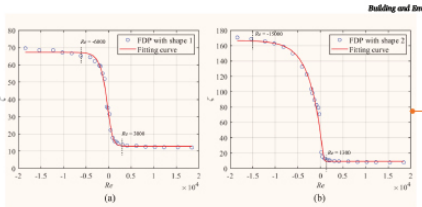

Fig. 10. Curve fitting results of the minor loss coefficients for FDP with Shape 1 (a) and Shape 2 (b) under forward and reverse flows at different Reynolds numbers.

Table 2
Function parameters in the logistic function Equation (8).

Parameters	A	B	C	D	S
FDP with Shape 1	62.25	-1.93×10^9	0.399	12.91	0.4654
FDP with Shape 2	149.1	-8.46×10^9	6.314	8.17	0.0416

Table 3
Simulation cases.

Cases	Shape of FDP	Direction of FDP	Reference wind speed at the building rooftop U_{ref} (m/s)
Case 0	No FDP	–	4
Case 1F	Shape 1	Forward	2, 4, 6, or 8
Case 1R	Shape 1	Reverse	2, 4, 6, or 8
Case 2F	Shape 2	Forward	2, 4, 6, or 8
Case 2R	Shape 2	Reverse	2, 4, 6, or 8

Fig. 11. Building geometry with the full-scale dimensions of W = 4 m, H = 3.2 m, w = 1.84 m, and h = 0.72 m. The FDP can consist of either Shape 1 or 2.

model has two symmetric openings located at the center of opposite walls. The wind direction is normal to the openings, and the airflow is expected to produce significant cross-ventilation in the building. In the other two cases, an FDP is installed at the opening on the windward wall. When the forward direction of FDP is along the approaching wind, this scenario is called the "forward direction"; when the forward direction of FDP is opposite to the approaching wind, it is called the "reverse direction."

A total number of 17 simulations were conducted in this study, as listed in Table 3. They include the cases with or without the FDPs, those under forward or reverse direction if an FDP is involved, and cases with different reference wind speeds at the building rooftop (U_{ref}). Notably, in the case without an FDP, the indoor ventilation rate should be proportional to the reference wind speed when the outdoor Reynolds number ($=HU_{ref}/\nu$) is sufficiently large; however, it is no longer proportional when an FDP is installed because the pressure loss brought by FDP is not proportional to the dynamic pressure, shown in Equation (9). Therefore, only one reference wind speed is considered in the case with no FDP, while multiple reference wind speeds are considered when an FDP is installed at the opening.

5.2. Simulation setup

The simulation domain and mesh grid are shown in Fig. 12. The building was located in a wind tunnel with a width of 48 m (=12W or 15H) and a height of 19.2 m (=6H). The inlet and outlet of the tunnel are 24 m (=7.5H) and 40 m(= 12.5H), respectively, from the center of the building. The domain size adhered to the recommendations outlined in the guidelines by Tominaga et al. [52].

The indoor and outdoor meshes are generated in two closed spaces. In general, the minimum cell size was 0.04 m (=W/100), which was adjacent to the building walls and openings, and the maximum was 0.64 m, which was adjacent to the tunnel walls. The total cell number is approximately 4.3 million.

The interfaces of indoor and outdoor meshes are walls and openings (see Fig. 12 (b)). The surfaces of both sides are set as the wall boundaries using the wall function of Spalding's law [43]. The same wall boundary setting is imposed on the floor. For openings with no FDP, the two surfaces of both sides are connected by a "cyclic" boundary condition in OpenFOAM, which directly maps all the physical quantities on the two sides of the interfaces.

When an FDP is installed at Opening 1, a self-made boundary condition is compiled and used in OpenFOAM. All other physical quantities are directly mapped as the cyclic boundary except for the pressure in this boundary condition. A pressure drop (i.e., ΔP, the outdoor-indoor pressure loss at the opening interface) is specified according to Equations (5) and (9), which is determined by the normal speed of the flow through that interface (i.e., the quantity V in Eqs. (5) and (9)). The normal speed is positive when the forward direction of FDP is along the approaching wind and negative when the forward direction of FDP is opposite to the approaching wind. In a CFD solver, the pressure drop and normal speed are coupled and solved iteratively. For example, according

8

Figure 4: After running simulations on two units of the best performing valves, Hu et al. (2024) mathematically formulated their performance to approximate their performance curves (Hu et al., 2024).

Section 7

Numerical method

This chapter will propose a quantitative model that can serve as an early indicator of the performance of different FDPs and replace time-consuming simulations. This model can ultimately help engineers and architects in determining the dimensions and parameters of Tesla Valves integrated within FDPs, thereby enabling the swift optimization of FDPs to suit any natural ventilation strategy. Formulas 5, 4, 13 and 15 form the basis of the model. The parameters are chosen to reflect the simulation setup of that of Hu et al. Additionally, a standard grill with similar specifications to that of the FDPs is modeled to compare their regulating performances. The calculations are performed using Python. The code can be found in Appendix 1.

7.1 wind pressure

The main objective of FDPs is to regulate the strongly variable inflow of are due to changing winds, which cause significant changes in pressure over a building's facade. The pressure difference across a facade typically ranges around 10 Pa but can increase to 400 Pa or more. On top of that, due to the winds varying nature, pressure differences can fluctuate considerably within a small time span (up to a factor of 2.5 within a frame of seconds) (Pleysier & Vos, 2017). The force of the wind on a building's facade or roof is contingent upon the speed of the wind and can be approached with the following formula (van Herpen, 2005).

$$\Delta P_w = \frac{1}{2} \cdot \rho \cdot C_p \cdot v^2 \tag{15}$$

ρ = air density
C_p = wind pressure coefficient
v = wind speed

The wind pressure coefficient is a factor by which the pressure determined from the wind speed at reference height is multiplied to determine the wind pressure on a building's façade or roof. This factor depends, among other things, on the building height, building shape, terrain roughness (open terrain, forest, or urban areas, which can be low-rise or high-rise), as well as the direction of the wind in relation to the facade. (Pleysier & Vos, 2017). Common values can be found in (Cauberg, 2013) and (van Herpen, 2005). The wind speeds that act at the heigh of an inlet are also influenced by multiple factors. these are captured in formula 16, with its parameters listed in table 9.

$$v = v_m \cdot K \cdot z^a \tag{16}$$

v = Wind speed at height of inlet[m/s]
v_m = Reference wind speed at 10 m[m/s]
K = Terrain roughness parameter [–]
z = Height above ground [m]
a = Exponent [–]

7.2 Parameters

To match the exact reference speeds of those used by Hu et al,, the reference speeds are set to be 0 to 8 meters per second. These are taken to be the air speeds with which the air exudes pressure on the facade. This means that the formula 16 will be ignored. The

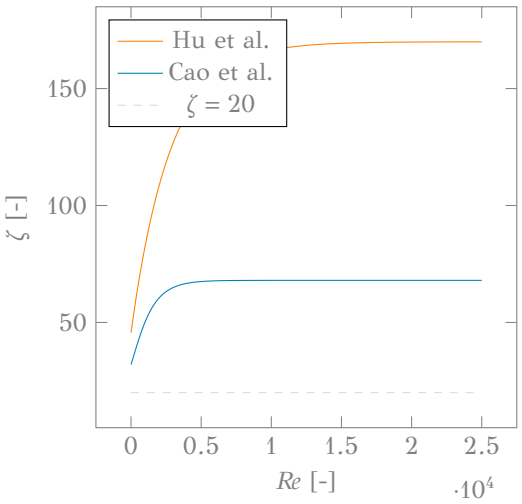

Figure 5: Minor loss coefficients for Cao et al. (2020) and Hu et al. (2024) with $a = 0.3125$ and the reference grille with $a = 0.3$ and $\zeta = 20$

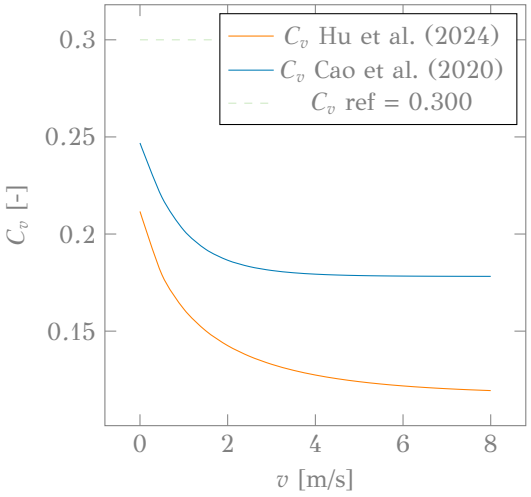

Figure 6: C_v as a function of wind speed

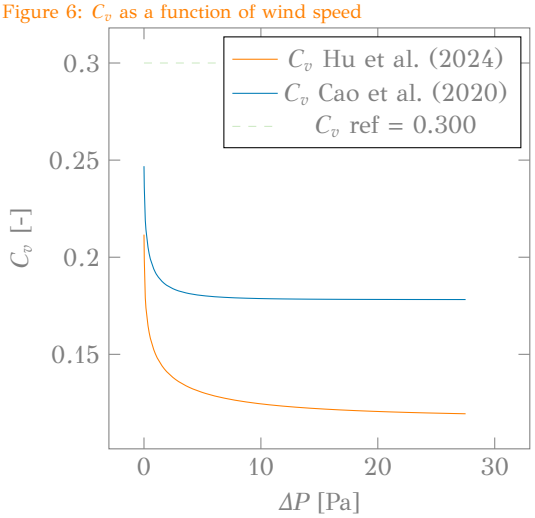

Figure 7: C_v as a function of wind pressure

Terrain type	K	a
open flat terrain	0.68	0.17
rural area	0.52	0.20
urban area with low rise	0.35	0.25
dense urban area with high rise	0.21	0.33

Table 9: Terrain coefficients for the Netherlands (van Herpen, 2005)

wind pressure coefficient is taken from (van Herpen, 2005) and is chosen to mimic the situation of the last set of CFD simulations of Hu et al, where the wind direction is normal to the surface of the FDP, in an open flat terrain. This is captured in a wind pressure coefficient of $C_p = 0.7$ to represent the positive pressure caused on the windward facade and $C_p = -0.5$ to represent the negative pressure on the leeward facade. The total pressure difference over the facade containing the FDP also depends on the inside of the building, which is generally taken to be the average between the value of C_p of the windward facade and that of the leeward facade(Rijksgebouwendienst, Bureau Bouwfysica, Afdeling Onderzoek en Ontwikkeling, 1984). Therefore C_p will be set as 0.6, following 0.7 - (0.7 - 0.5) / 2.

Furthermore, when modeling the inlet to obtain its C_v as per equation 4, it is modeled as a square gap in a wall with the same dimensions as that in the simulation, which are 1840 mm (width) and 720 mm (height), resulting in a hydraulic diameter of $D_h = 1.035$ according to equation 7. The inlet is modeled to be 0.4m deep, with the FDP as an independent element with its minor loss coefficient modeled as its performance curve. The porosity, a, used during the simulations to obtain the performance curves of the FDPs was 0.3125. The reference grille will therefore be modeled as a standard grille with a porosity of 0.3 and a minor loss coefficient of $\zeta = 20$ as per table 7.All parameters used to run the model are listed in table 10

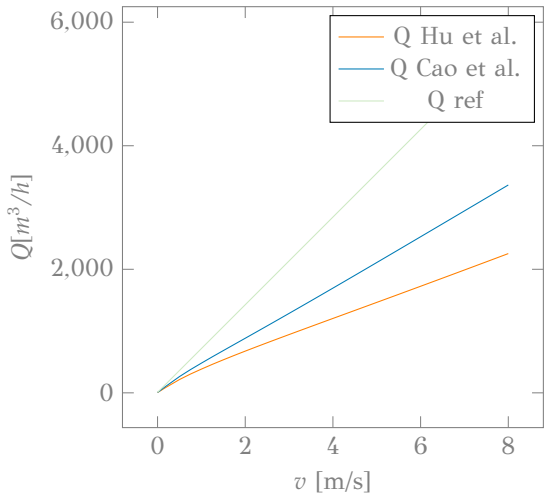

Figure 8: Q as a function of wind speed

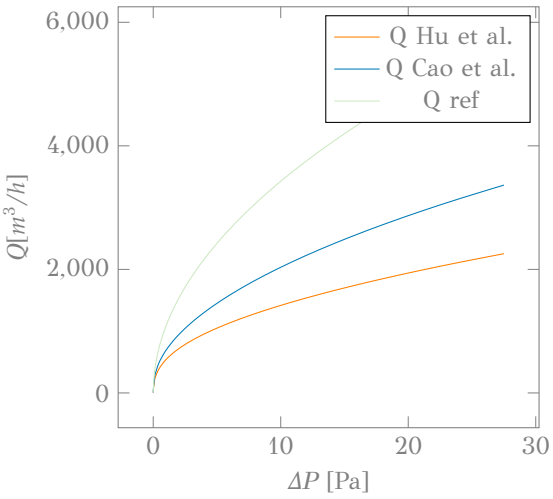

Figure 9: Q as a function of ΔP

7.3 Model verification

To compare the numerical method to the CFD simulations, the objective is to obtain the normalized volumetric ventilation rate as formulated in equation 14. For that, the volumetric ventilation rate (equation 5) has to be calculated, which in turn requires the wind pressure and the flow coefficient of the set-up to be calculated. Firstly, to obtain the resulting pressures for wind speeds from 0 to 8 meters per second, equation 15 is used. To obtain C_v, equation 4, is used. As stated in chapter 7.2, instead of using a constant to represent the minor loss coefficient over the FDPs (as is the case with the standard reference grille), the performance curves of the FDPs are used. The result of this can be observed in figure 7, which shows that C_v decreases significantly for both the Tesla valves with higher wind speeds. This confirms that with higher wind speeds, the FDP facilitates a significantly lower airflow, while C_v of the standard grill is constant (namely $C_v = 0.227$). It is also clear that compared to the standard grille, the FDP is less capable of facilitating air flows at lower speeds, which might be a problem for natural ventilation without any mechanically induced additional pressure differences, as explained in chapter 5.1.1.

Plotting the volumetric ventilation rate using equation 5 and the values for C_v in figure 9 shows the theoretical performance of the FDPs. The regulating properties of the Tesla valves can be observed in comparison to the standard grille. Furthermore, the large difference in C_v between the standard reference grille and the valves at low speeds can be observed, as the ventilation rates already differ significantly at 1 Pascal. It should be noted that this scenario mimics that of the simulation of Hu et al., who worked with a large FDP ($A = 1.325\,\mathrm{m}^2$). Therefore, the ventilation rates are large as well. However, achieving a realistic ventilation rate is not the main objective of the simulation or this chapter. Instead, the focus is on comparing the normalized volumetric ventilation rate, To understand the FDPs performance regardless of their size, which allows for comparison between different FDP models, calculation and simulation methods. Chapter 10.2 will focus on performance in a practical scenario. The volumetric ventilation rate can now be normalized following equation 14 to directly compare the output of the numerical approach with that of the simulation with that of Hu et al. The results are plotted in table 11.

The plot clearly shows that the numerical method shows similar behavior to that of the simulations. However, it estimates a lower volumetric ventilation rate than the CFD. A possible reason for this is the value for the wind pressure coefficient C_p for calculating the wind pressure (equation 15) has been chosen too low. $C_p = 0.6$ resulted from the assumption that the pressure inside the building was the average of the two pressures working on both facades. This can however be influenced by openings in the walls. The indoor pressure can be higher than the average air pressure if, for example, there is an opening on the windward facade, or lower if there is an opening on the lee side of the building (where the wind pressure is negative). (Pleysier & Vos, 2017). In the case of the simulation of Hu et al., there are two identical openings on opposite sides of the building, of which only the one facing the wind is fitted with a regulating FDP. This means that the suction effect of the wind might create a lower indoor pressure, causing an overall larger pressure difference over the facade with the FDP, resulting in a situation where C_p will be presented better by taking the total pressure difference over the building, which would be reflected in a C_p of 1.2. The results of running the calculation with a C_p of 0.9 and 1.2 are shown in figure 11.

This improves how well the model estimates the performance of the FDPs. The remaining differences between the simulation and the calculation might be explained by wind phenomena around the building which can be simulated accurately in CFD analysis

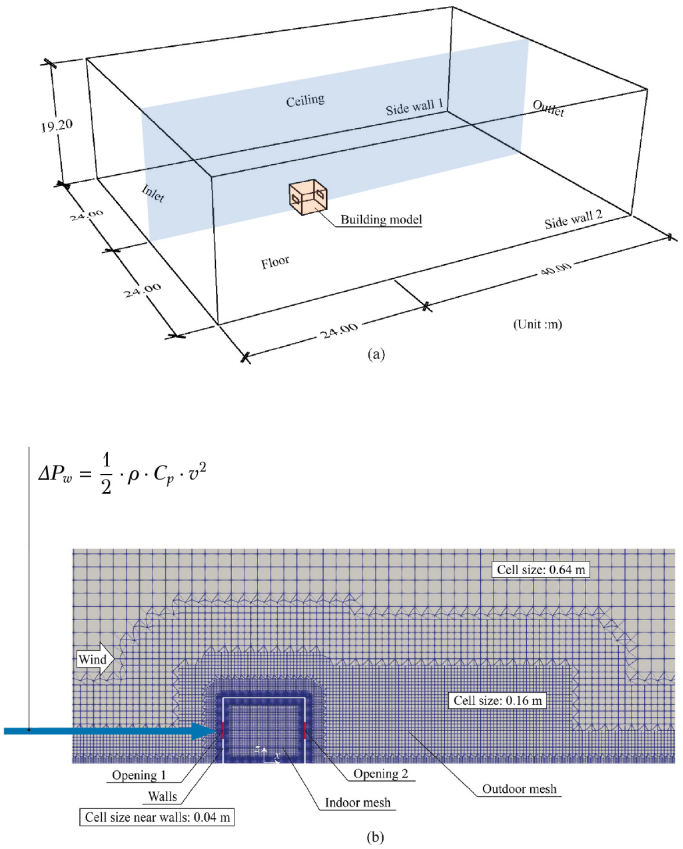

Figure 10: After running simulations on two units of the best performing valves, Hu et al. (2024) mathematically formulated their performance to approximate their performance curves (Hu et al., 2024).

but can not be captured sufficiently in the single values of C_p. Despite the slight deviations from the CFD simulations, the model is accurate enough to estimate an FDP's performance, as long as their performance curve is known. Obtaining the performance curve however still can only be achieved through simulations. This issue will be discussed in chapter 11

7.4 conclusion

As of yet, the results of the proposed numerical model do not fully match with the CFD results from Hu et al (Hu et al., 2024). Potential ways to improve its accuracy are discussed in chapter 7.3. However, the objective of the model is to quickly determine what valve and FDP specifications suit a given situation, as was recommended by Cao et al(Cao et al., 2020). A way of how this model can do so will be explored in chapter 11. Its function as such means that it does not need to be as accurate as a CFD analysis. However, the model is worth improving upon regardless.

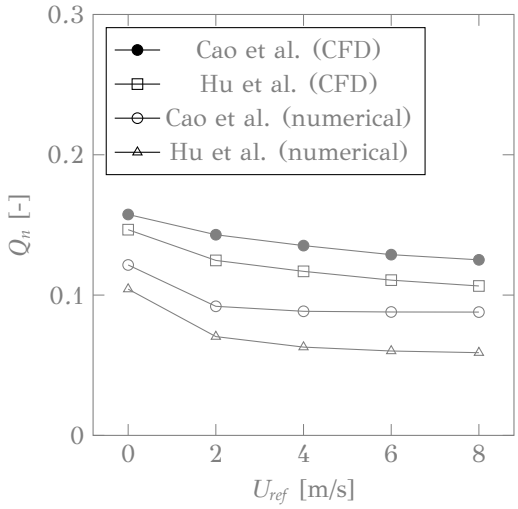

(a) for C_p = 0.7 (A)

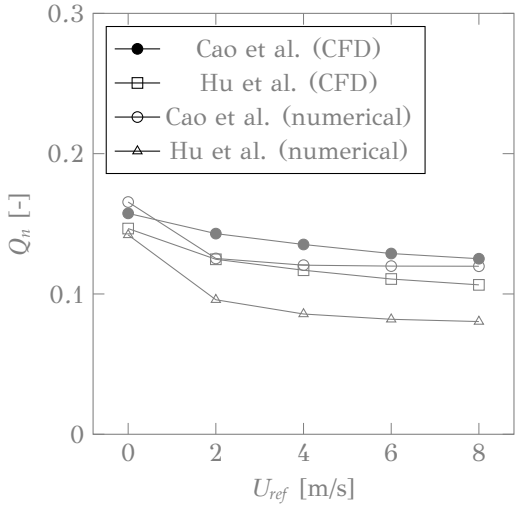

(b) for C_p = 1.2 (B)

Figure 11: Combined plots of Q_n for different values of C_p

formula	element	Parameter	Value
15	C_p	Terrain	open flat terrain
		Wind angle	0°
		Wind Pressure coefficient	0.6
-	v_ref	Wind speeds (v)	[0 - 8] m/s
12	Re	v (kinematic viscosity air)	$1.5\dot{1}0^{-5}$ [kg/(můs)]
		a (porosity)	0.3125 [-]
4	C_v	Inlet width	1.840 m
		Inlet height	0.720 m
		A_{inlet}	1.325 m^2
		D_{hinlet}	1.035
		l_{inlet}	0.4 m
		λ	0.045 [–] (van Herpen, 2005)
		ρ_{air}	1.225 kg/m^3
	$\Sigma\zeta_i$ (FDP)	ζ of FDP	performance curves (equation 13)
	$\Sigma\zeta_i$ (ref)	ζ grille with $a = 0.3$	20
5		n	2 (representing a fully turbulent flow)

Table 10: An overview of all parameters used for the calculations

Section 8

Test case manufacturing

The motivation to research FDP as a case study for how AM might be unlocked by designing passive, resilient, and multi-functional building parts was explained. This chapter will assess its suitability for 3D printing.

8.1 Suitability

What makes FDPs particularly suitable for AM is their need to be customized to specific scenarios as explained in chapter 6.2. FDPs on higher floors will require a higher regulating capability than those on lower floors. Their strength also lies in the fact that they can be fitted in any inlet of any dimension. Customizability, an essential strength of 3DP, is therefore a necessity for FDPs to function. Additionally, due to their complex shape and small dimensions (especially when it comes to the baffles), 3DP seems the most suitable method of manufacturing. On the other side, in their most basic form, FDPs are essentially repeated extrusions. This means that, especially in the case of mass production, standard extrusion methods cannot be excluded from feasibility studies.

8.2 test case

To test both the performance of the FDP and its manufacturability, A small FDP was created using a parametric model (which is explained in depth in chapter 11.1.2). Its dimensions are 60 mm (W) x 85 mm (H), containing four rows of Tesla valves with four flow loops, of which the dimensions are that of the optimized valve by Hu et al. (see table 6) (Hu et al., 2024). The resulting depth of the FDP is 70 mm

To speed up and simplify the printing process, the baffles are not printed. Instead, they are manually cut from 1mm cardboard and inserted through openings in the side of the FDP. This was done after finding that the baffles caused some issues during printing (see chapter 8.3.1). To further simplify the printing process, the FDP was printed in two mirrored halves, which were then attached to form a functional FDP.

8.3 methods

For the printing of the FDP, two methods of 3D printing were explored, namely masked stereolithography (MSLA), which is a form of SLA printing, and fused deposition modeling (FDM).

MSLA is an additive manufacturing process that uses photopolymer resins to create 3D objects layer by layer. The material used when resin printing is a liquid resin that hardens when exposed to a specific type of light is used as the primary material, and a light source, such as a laser (called SLA) or a projector (MSLA), selectively exposes the resin to light according to the pattern of each layer. Wherever the light hits the resin, it undergoes photopolymerization, transforming from a liquid to a solid state. This process is repeated layer by layer until the entire object is formed(Rashid et al., 2020). the advantage of MSLA over SLA printing is that the throughput (the rate at which it prints objects) is much higher, due to its ability to cure entire layers at once. This means only the amount of layers matters, not the surface area of the objects and as such, multiple objects can be printed simultaneously without an increase in printing time (Solidator, 2023).

FDM (Fused deposition modeling) on the other hand is an Extrusion-

based additive manufacturing (AM) method, which uses a nozzle to extrude a viscous material stored in a reservoir. Upon extrusion, the material solidifies, adhering to previously deposited layers. In the case of FDM, polymer filaments are used, which are melted in a heating chamber and extruded through a nozzle under pressure. FMD is among the most widely adopted AM methods(Rashid et al., 2020). Table x compares the general performance between the two (Formlabs, n.d.) (Formlabs, n.d.) (Solidator, 2023).

Aspect	FDM	MSLA
Resolution	●●○○○	●●●●●
Accuracy	●●●●○	●●●●●
Surface Finish	●●○○○	●●●●●
Throughput	●●●○○	●●●●●
Complex Designs	●●●○○	●●●●○
Ease of Use	●●●●●	●●●●●

Table 11: Comparison of 3D Printing Technologies (Formlabs, n.d.)

8.3.1 test prints

The first attempt to print the model was done using MSLA. At this point, the test model still had baffles, as theoretically, MSLA should be able to fastly (Due to its ability to print multiple objects at once) and accurately print such small details. However, despite its theoretical ability to print the FDP, all the attempts made during this research failed. Despite that, this technology is very promising for feasible and fast production of FDPs. There is however a big disadvantage of resin printing, namely that the resins used for this technology are often toxic, which does not align with the objective of this paper to create resilient solutions (Griffin, 2024).

The quality of the FDM prints is far better. On top of that, especially compared to resins, PLA is more environmentally friendly, as it is bio-plastic. However, it still requires special attention for recycling or composting (Filamentives, n.d.).

8.4 Conclusion

From the two 3D printing technologies explored in this chapter, it is clear that for efficient and large-scale production of FDPs, MSLA is the most suitable method. Based on the trials, however, it has also become clear the FDP design would have to be optimized to this particular 3D printing method, which requires further research. Further research in this paper will use FDM printing, as, despite its inferior specifications, it has proven to be very suitable, both quality and speed-wise, for the scale this paper works with. A conclusion on what is the most effective printing method on a larger scale will be drawn in chapter 12

Figure 12: The MSLA (upper) and FDP test prints (own work)

Section 9

Test

9.1 Set up

The test was designed to simulate wind blowing on a facade. This was done by placing the 3D-printed FDP in the middle of a 500 mm by 500 mm plate. The FDP is made up of the two printed halfs, glued together and fitted with baffles manually. Its dimensions are 60 mm x 85 mm, with the baffles being around 1 mm thick. The internal valves are that of Hu et al. (2024) (Hu et al., 2024) with the same porosity of 0.3125. However, due to the smaller dimensions of the printed FDP, in practice, the porosity is somewhat lower, as the amount of closed area is relatively large compared to the small amount of open area. Additionally, a standard grille of the same dimensions was made as a reference. Lastly, a channel with the dimensions of the FDP holds the FDP and allows for accurate measurements of wind speeds in the channel.

The setup is designed in such a way that the FDP connects the large plate and the channel. Just above the FDP, a small inlet is created for a pressure meter (the Testo 400), registering the pressure exerted on the facade by a small ventilator. Within the channel, an Extech hot wire CFM Thermo Anomonemeter was placed to measure the wind speed. This allows the wind speed in the channel to be plotted against the pressure difference over the FDP, which can be compared to the outcomes from the calculations. The measurements were done at 4 distinct speeds of the fan.

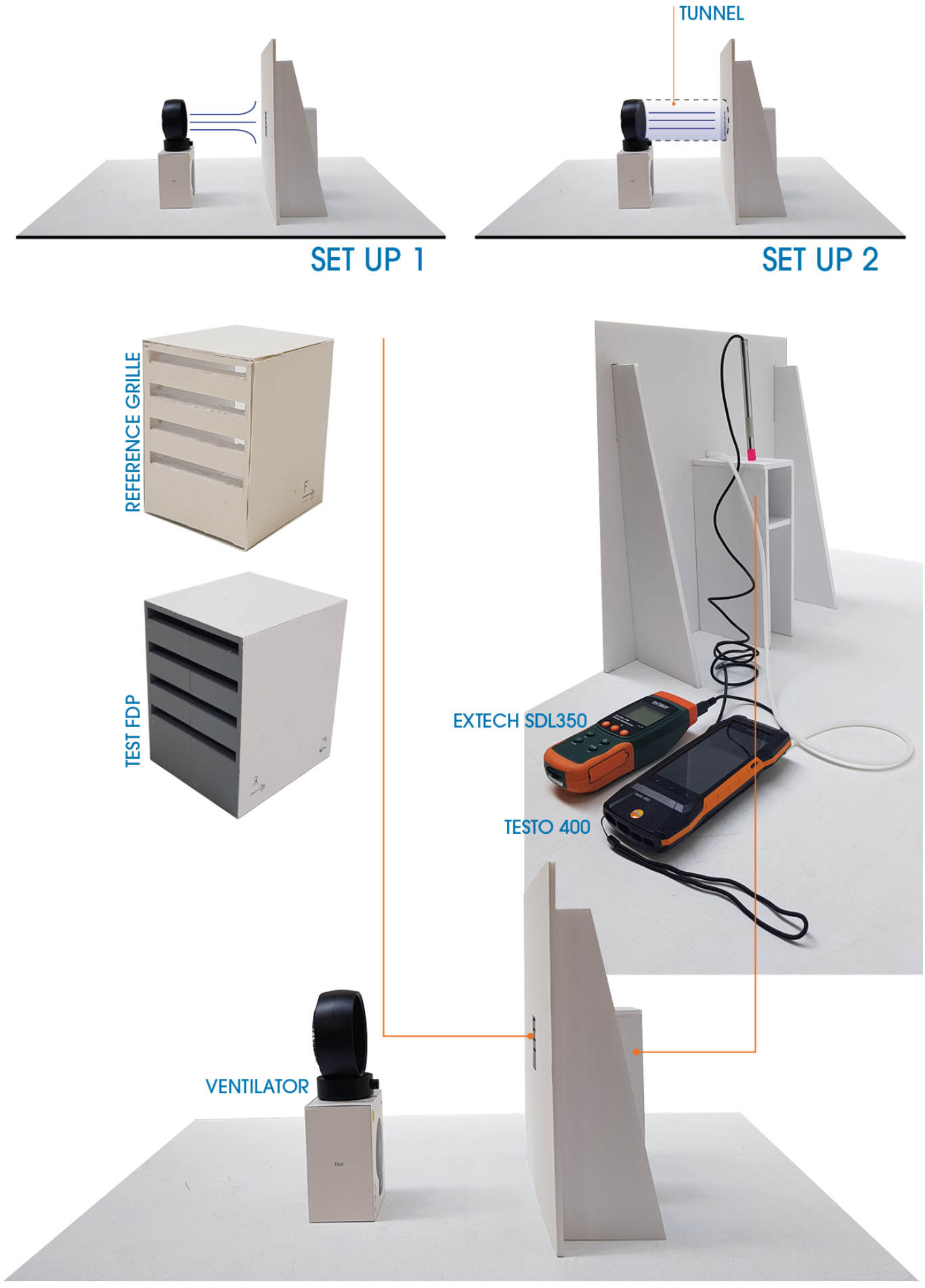

Figure 5: The test set up (own work)

9.2 Results

Initially, the test setup was designed to mimic wind blowing on a facade (see 5). However, too many parameters were influencing the measurements. This brief exploration did however make clear that the behavior of the FDP is very sensitive to external factors, meaning that to verify its performance, it will have to be tested in a real-life scenario. To better mimic the experiment as done by Cao et al. (2020) (Cao et al., 2020), which is the foundation of all further simulations both by them and by Hu et al. (2024) (Hu et al., 2024), the ventilator was placed in a cardboard channel with the same diameter, which was placed against the FDP. This created a reliable environment for measuring.

The first step was to determine the right value for the porosity, which was done by testing the standard grille (figure 6). It was found that their result matched that of a grille with a resistance of $\zeta = 0.25$ (which is slightly higher than a grille with a porosity of $a = 0.3$ with a minor loss coefficient of $\zeta = 0.2$).

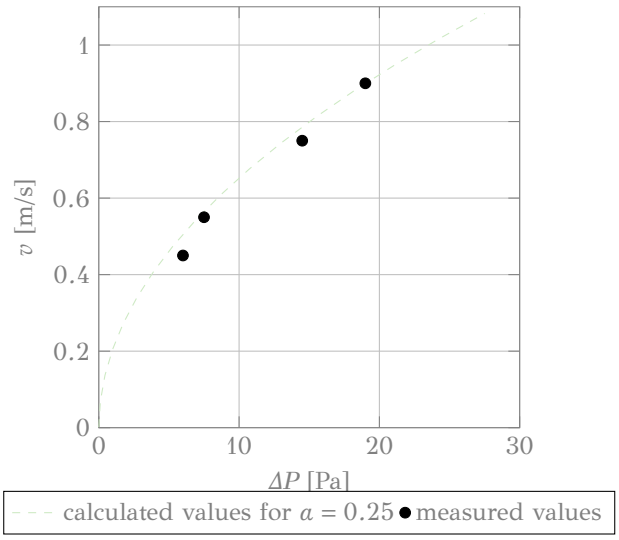

Figure 6: The first measurement determined what calculating value for the porosity of the grille and FDP should be used

With the new test setup, the FDP performed significantly better. It did however still not perform reliably. slight differences in how the tube was positioned against the FDP resulted in a large variance in speeds measured within the channel. However, when plotting the lowest wind speeds measured at each set of measurements (figure 7), we do see the FDP does add resistance compared to the standard grille, and most closely resembles the behavior of the FDP as proposed by Cao et al. (2020) (Cao et al., 2020), despite the FDP being modeled after the optimized version of Hu et al. (2024) (Hu et al., 2024).

Possible explanations for the performance not matching that of the simulation could be the fact that the baffles were inserted manually, instead of printed. However, Hu et al. (2024) (Hu et al., 2024) concluded in their research that smaller baffles would result in better performance. Another possible explanation is that FDPs are sensitive to external factors such as wind direction and how laminar the incoming airflow is. The performance curves are simulated with a laminar flow as input. In reality, this will rarely ever be the case.

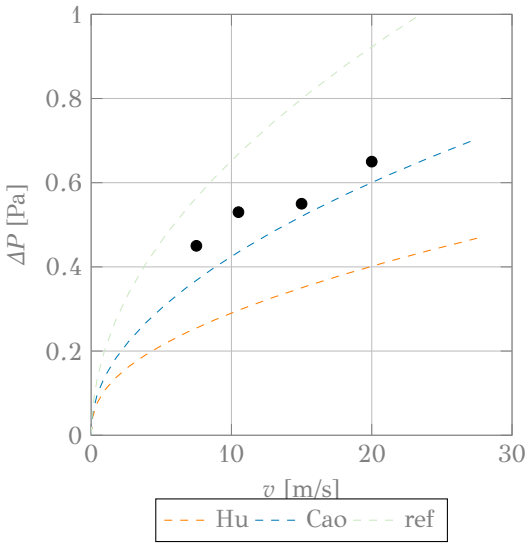

Figure 7: The lowest measured wind speeds in the channel do approach the behaviour of the simulations of Cao et al. (2020)

9.3 Conclusion

As such, the tests has shown that FDPs can perform according to CFD simulations, albeit with lesser performance than simulated. Additionally, slight changes in external conditions can drastically influence its regulating capabilities. To make FDPs function as optimal as possible, the conditions of the simulations should be mimicked as much as possible, meaning the inlet design should facilitate the creation of laminar flows as much as possible. This can be achieved by avoiding sharp transitions within background ventilators, creating a smooth entrance into the inlet instead (van Herpen, 2005). which limits the creation of turbulence in the airflow before it hits the FDP.

Section 10

Performance

10.1 Performance indicators

Chapter 5.3.1 discussed the regulations around background ventilators. For natural ventilation, a sufficient ventilation rate has to be able to be provided by the inlet with a pressure difference of 1 Pa. A background ventilator's efficiency is also often expressed as its capacity over 1 Pa difference. This is essentially the flow coefficient of the background ventilator, as explained in chapter 6.4.1. However, since FDPs offer higher resistance at higher pressure differences, meaning its C_v is not a constant, it is difficult to compare FDPs as such. On top of that, What is considered a sufficient ventilation rate differs per situation, and is determined among others by the floor area of the room the BV has to serve, as well as the number of people that that room is expected to house. As a rule of thumb, however, a ventilation rate of 25 m^3/h per person should be easily obtained. Ideally, it should be able to provide two people with fresh air, requiring roughly 50 m^3/h. When working with type C ventilation, a pressure difference of 5 Pa can be assumed (Nijeboer & Hage, n.d.).

10.2 Performance

The numerical model will be used to estimate the performance of background ventilators fitted with FDPs. To do so, they will be compared to the Duco Silenzio, which delivers 9 dm^3/s ($9 \cdot 10^{-3}$ m^3/s) of fresh air over a pressure difference of 1 Pa. Using formula 4 gives that this means the sum of minor loss coefficients $\Sigma\zeta_i$ equates to a mere 1.65. This seems exceptionally low, as theoretically at least, the sum of minor loss coefficients of a cap and a grille in front of an inlet should equate, at least in theory, to at least 2.5 (van Herpen, 2005). Despite that, the Silenzio offers a good baseline for comparison.

The Silenzio has a diameter of 250 mm. However, due to the acoustic lining, the channel through which air can flow is rectangular and measures 130 mm by 130 mm. The BVs with the FDPs are modeled with these dimensions as well. Figure X shows their respective C_v. The FDPs cause significant resistance, also at low-pressure differences. The result of this is that the inlets with the FDPs are unable to reach a sufficient ventilation rate, nor with 1 Pa, nor with 5 Pa, whereas the Duco Silenzio can provide sufficient ventilation for two persons at a pressure difference of 2 Pa. It should be noted that the regulating abilities of the Silenzio are not taken into account in this plot.

The most effective way to increase the ventilation of the BVs containig the FDPs is to increase their area. The result of increasing the area of the inlets to 200 mm by 200 mm is plotted in Figure Y. The results show a performance that is more suitable for practical applications. Although This means increasing the area of the inlet with 42% , it is important to note that the total diameter of the Duco Silenzio is 250 mm, as it has to accommodate the insulating lining for sound absorption. If the FDP can be designed to insulate sound sufficiently well that the lining becomes redundant, the dimensions of the inlets could stay more or less the same.

Lastly, the resulting wind speed in the channel is plotted in Figure Q. Here, the strength of the FDP becomes apparent. Theoretically, the FDPs should be able to keep the speed in the inlet under the allowed 0.2 m/s up to wind speeds of 4 m/s. These are the speeds with which the wind hits the facade of the building. Figure L shows that speeds of this kind or lower make up around 30%

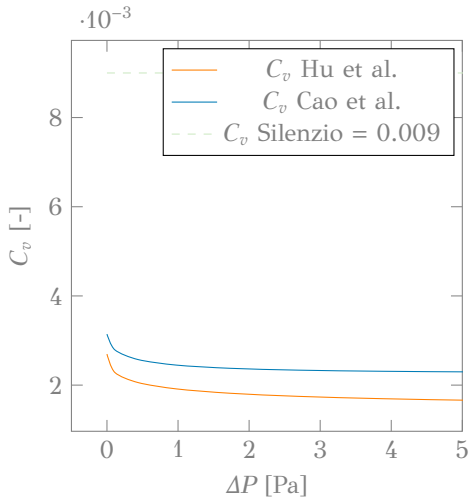

Figure 8: C_v as a function of wind pressure

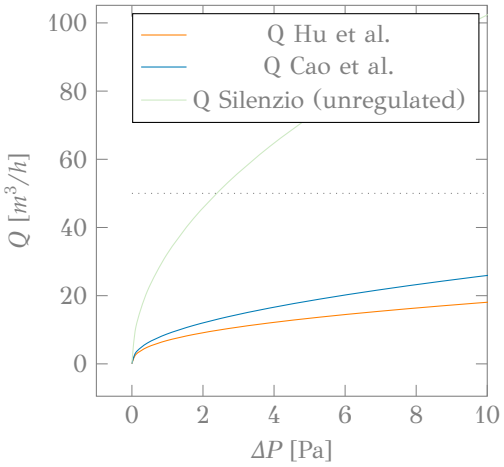

Figure 9: ventilation rate for ΔP. The vertical line at ΔP represents the lower limit at which inlets are expected to provide enough ventilation in a natural ventilation scenario

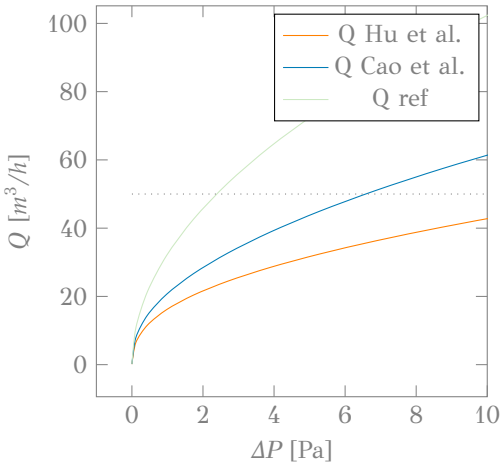

Figure 10: ventilation rate for ΔP. To reach a ventilation rate of 50 m^3/h at 10 Pa, an area of 200 by 200mm is required.

of occurring wind speeds in the Netherlands. However, these wind speeds than have to be converted to wind speeds applicable to the context, according to formula 16, meaning, in reality, this percentage will be higher.

10.3 Conclusion

In its current form, the FDPs provide too much resistance at low pressure differences to be suitable for application in naturally ventilated buildings.

The objective of this chapter was to numerically if FDPs offer enough passive control over the inflow of air at higher wind speeds, making the need for closing mechanisms redundant. The outcome of the model shows this is not yet feasible. Instead, the maximum allowable speed of 0.2 m/s is already reached at wind speeds of around 3 m/s. This estimation is still generous, as the numerical model overestimates the performance of the FDP. It is however significantly better than a standard grille of the same porosity. The easiest way to improve the performance of the FDPs is by adding additional valve units, as demonstrated by Cao et al. However, this will also increase its resistance at low-pressure differences, which is undesirable. It should also be repeated that the configuration as proposed by Hu et al. is not the most optimized valve thinkable. Chapter 11 will review the possibilities for further optimizations. Alternatively, the performance can be improved by adding caps to the BV to block the most direct wind, as is common practice. At low wind speeds, the FDPs behave similarly to normal grilles. This is desired since natural ventilation systems are expected to function at low-pressure differences. The FDP does however add resistance even at low wind speeds. Taking all this into consideration, the concept of FDPs to regulate NV is a feasible one, at least when it comes to its performance. The rest of the thesis will focus on the feasibility of the FDPs when it comes to their manufacturing.

Optimize towards less resistance at low speeds, regulating behaviour only at higher wind speeds

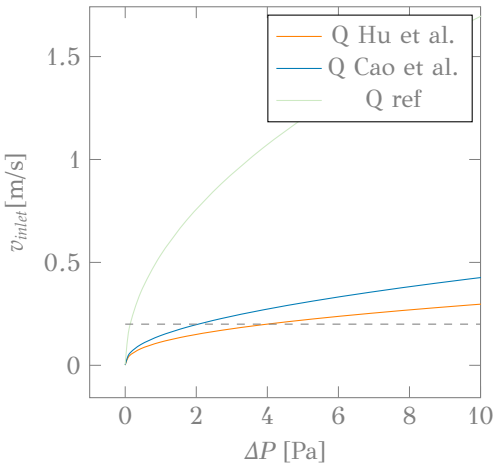

Figure 11: ΔP as a function of wind speed for $C_p = 0.7$

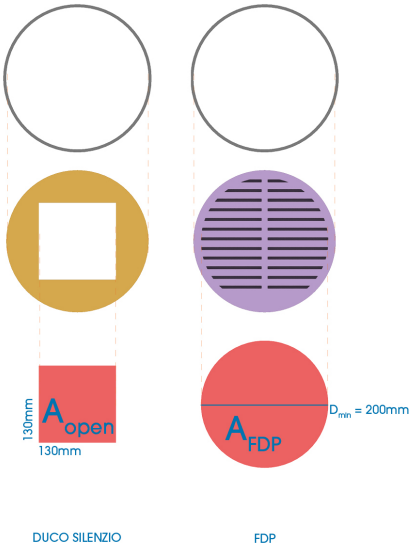

Figure 12: For the FDP to allow enough fresh air it requires a larger area compared to a standard inlet

Section 11

framework

This chapter will investigate how the numerical model can be implemented into a predictive model to allow efficient selection of the right Tesla geometry to meet particular requirements of a project. To do so, however, an efficient way to obtain the performance curves of a Tesla valve is required. As of current, there is no way to obtain the performance curve of a Tesla valve other than through CFD analysis or AI predictions. The goal of this chapter is to provide an overview of the optimization possibilities of Tesla valves and to efficiently obtain their performance curves.

11.1 Optimization

Throughout this research, the following objectives have been identified for the optimization of Tesla valves for their application in NV. These are 1) to provide as little resistance as possible at low wind velocities and 2) to provide as much resistance as possible at high wind velocities. The latter will influence how many flow loops will be needed to achieve the required regulating properties. With optimized valves, fewer flow loops will be required, reducing the thickness and material needs for the FDP. It also reduces the resistance the FDP offers in the forward direction. This is however of lesser importance. However, optimization possibilities are restricted for reasons discussed in chapter 6.2.

Optimizing Tesla valves can be done in multiple ways. Much research has been done to find the optimal parameters for the traditional Tesla valve, either through CFD analysis (Cao et al., 2020) (Hu et al., 2024) (Bao & Wang, 2022) (Zhang et al., 2023) or through the use of machine learning methods, as was done by Peng et al. (2023) using multi-layer perceptron models (Peng et al., 2023). Other research has found alternative shapes and layouts for the Tesla valves to improve its performance significantly. Fadl et al. (2009) researched the efficiency of multiple valve structures, including the conventional Tesla valve, focusing specifically on their performance at very low Reynolds numbers(Fadl et al., 2009). Liu et al. (2022) researched the performance of symmetrical Tesla valves compared to that of traditional ones, concluding they perform significantly better (Liu et al., 2022). The limiting factor of these variations on the Tesla valve is that they stack less efficiently, leading to less efficient integration into an FDP. The final method uses topology optimization to optimize the principle of the Tesla valve, which was done by Böhm et al. (2022) (Böhm et al., 2022). This results in completely different geometries entirely, which are not easily manufactured on a large scale. On top of that, topology optimizations result in the optimal performance of the valve in a very specific setting, whereas the performance requirements change per application. Therefore, a more customizable valve design is preferred.

11.1.1 lattice Boltzmann method

A significant issue with all research regarding the Tesla valve is that their simulating them using traditional CFD methods is complex to set up and time-consuming. In the past 20 years however, a new simulation approach has rapidly gained popularity. The Lattice Boltzmann Method (LBM) is known for its ability to handle various types of flows and its simple approach to representing boundaries using binary masks, along with its easy parallelization and use of regular meshes. It has shown great promise in computational physics, especially in microfluidics (Fadl et al., 2009). Its strength LBM lies in the fact that, unlike conventional CFD

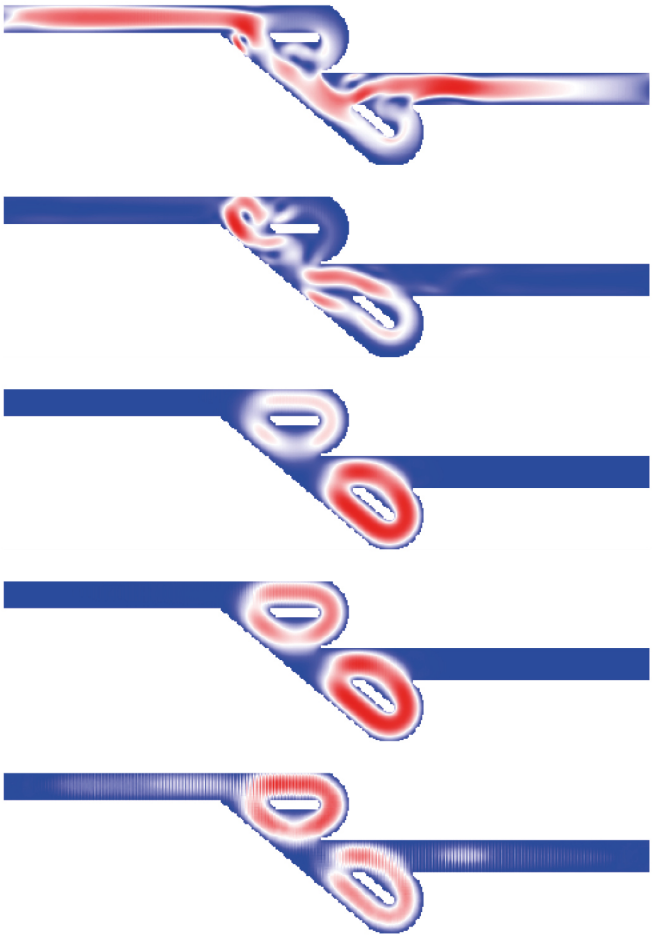

Figure 13: The Boltzmann implementation proves it is fast and easy to implement. However, more research is required before it can accurately mimic the behavior of flows in a Tesla valve

methods, LBM functions on a discrete lattice grid where individual nodes serve as computational points. Each node is associated with a distribution function, representing the probability of particle groups moving in defined directions and with what velocities (SimScale, 2023). Thanks to it easy parallelization, it allows for efficient utilization of computational resources and accelerated simulations of complex flow phenomena within Tesla valves. Additionally, BLM's lattice-based approach facilitates the representation of intricate geometries, enabling detailed modeling of flow behavior within the Tesla valve's asymmetric channels and side channels. Moreover, BLM inherently captures turbulence effects through its mesoscopic approach, providing insights into the flow patterns and energy dissipation mechanisms within the Tesla valve. Furthermore, BLM allows for adaptive mesh refinement strategies, enabling the resolution of flow features near-critical regions of the Tesla valve to enhance simulation accuracy. (Ganji & Kachapi, 2015). This means that BLM offers some important advantages that make it well-suited for efficiently simulating the efficiency of Tesla valves, which was proven by Fadl et al. (2009) (Fadl et al., 2009) by successfully implementing the Boltzmann method to study the performance of different types of Tesla valves.

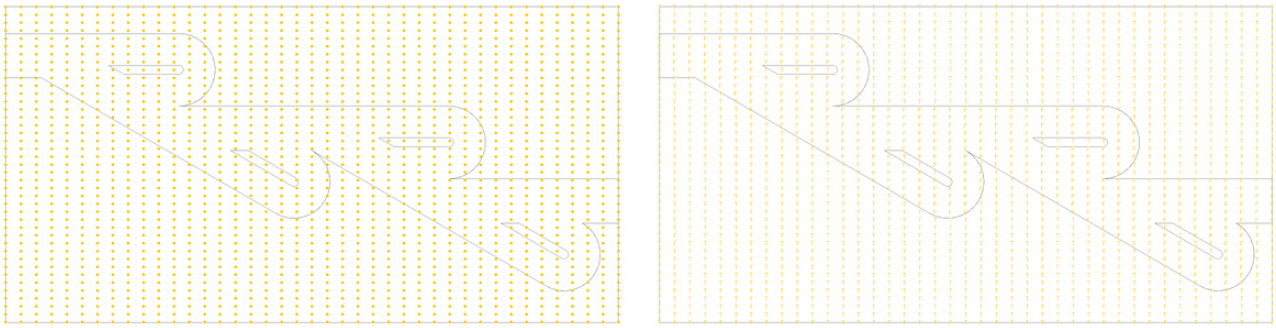

Figure 6: The binary mask of the Tesla valve (own work)

A possible way to obtain the performance curves for a vast amount of valves might be done as follows. In Grasshopper (Tedeschi, 2014), a parametric model generates a vast amount of Tesla valves within the ranges that were already identified by Hu et al. (2024) and summarized in chapter 6.1. A proposal on how this might be done is provided in chapter 11.1.2. Since the lattice Boltzmann Method works on a mesh grid and makes use of binary masks to represent boundaries, the resulting geometry from the first component ought to be translated to a mask. This is easily achieved by projecting a grid over the geometry and testing whether or not the grid points are in or outside the flow channel, resulting in a usable True/False mask. From this point it is recommended to move out of the Grasshopper environment, as it is rather slow and parallel computing is difficult to achieve. Additionally, external libraries used for the Boltzmann method are not (or difficultly) obtainable within grasshopper. Instead, Python is used to run the simulations. An efficient way to run the Python simulations from Grasshopper might be using the Hops plug-in (McNeel, n.d.), but this has not been attempted by the author due to time constraints.

To run the simulation, the only requirement is to load in the mask into the Python script. However, to exploit the Boltzmann method to its full potential, great attention should be paid to effective parallelization, as to obtain the performance curve, the simulations will have to be run at multiple speeds (and if desired, in both directions), in a similar way as done Hu et al. (2024), which means an optimized simulation method is required. Once a significant data set of performance curves has been selected, they can be integrated into a numerical model which allows for manual selection of the right performance curve (and thus the right valve) for a specific application. Additionally, they can be used to train machine learning models to predict or generate the right valve for a specific application. This is further explored in chapter 11.1.3. and is largely based on the works of Ortiz (2022) and Mocz (2022). The implementation of the Boltzmann method demonstrates that it is both quick and straightforward to execute. Nevertheless, further study is needed to precisely replicate the flow dynamics in a Tesla valve since in its current state it is not able to accurately mimic the results of the simulations of Hu et al. (2024) and obtain the performance curve.

11.1.2 parametric model

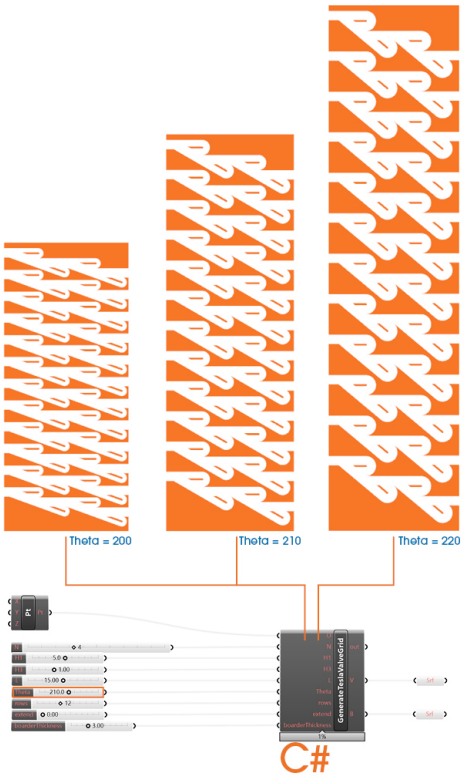

Figure 7: FDP generator (own work)

To run the Boltzmann simulations for multiple variations of the Tesla valve, a parametric model providing a binary representation of the Tesla valve is needed. This chapter proposes a simple method to rationalize and parameterize the Tesla valve using c# and grasshopper and generate its binary representation.

11.1.3 AI prediction

in chapter 3.1.2 it was mentioned that multi-criteria optimization results in higher resilience of building components.

Once a sufficient amount of CFD analysis have been run, the results can be used to train machine learning models to predict the optimal valve for any situation. This concept has been tried and proven in a couple of researches. First of all, Du et al. (2023) (Du et al., 2023) propose an artificial neural network (ANN) model that can predict and optimize the performance of Tesla valves based on specific application goals. Their study focused on hydraulic systems, where strong diodic characteristics are required from the valves, and on thermal management applications, where the valves had to be optimized to maximize convective heat transfer. Based on the different optimization objectives, the model was able to provide the most optimized valves. Although the optimization objectives for the FDPs are very different, a similar approach could be taken to optimize towards NV regulation. Vaferi et al. (2023) (Vaferi et al., 2023) proposed a similar strategy, predicting optimal designs of the Tesla valve for different conditions using a genetic algorithm method and prediction models. The results indicated that the coefficient of determination for both prediction models was above 0.99, demonstrating high accuracy(Vaferi et al., 2023)(Vaferi et al., 2023). Although these researches did not focus on Tesla valves in NV applications, their general structure might be adapted to do so.

Once able to predict how the number of units affects the efficiency of the FDP. Liu et al. (2022) provides a method to define such a scaling law. (Liu et al., 2022)

11.2 Conclusion

It can be concluded that the proposal for the optimization and selection method is for the most part an efficient and functional one. However, for it to work, some important steps still have to be made. Currently, the mathematical approach to the FDP's behavior mimics that of simulations well. It can be concluded with relative certainty that The Boltzmann lattice method would be the most suitable to realize bulk simulation to train a multi-objective AI model. However, the current implementation proposed in this paper is too basic to accurately depict the FDP's behavior and needs further development. Using the AI predictions and a fine-tuned mathematical model would provide a very useful tool, and should be explored further by solving the aforementioned shortcomings of the current implementations

PART 3

TOWARDS HOLLISTIC DESIGN

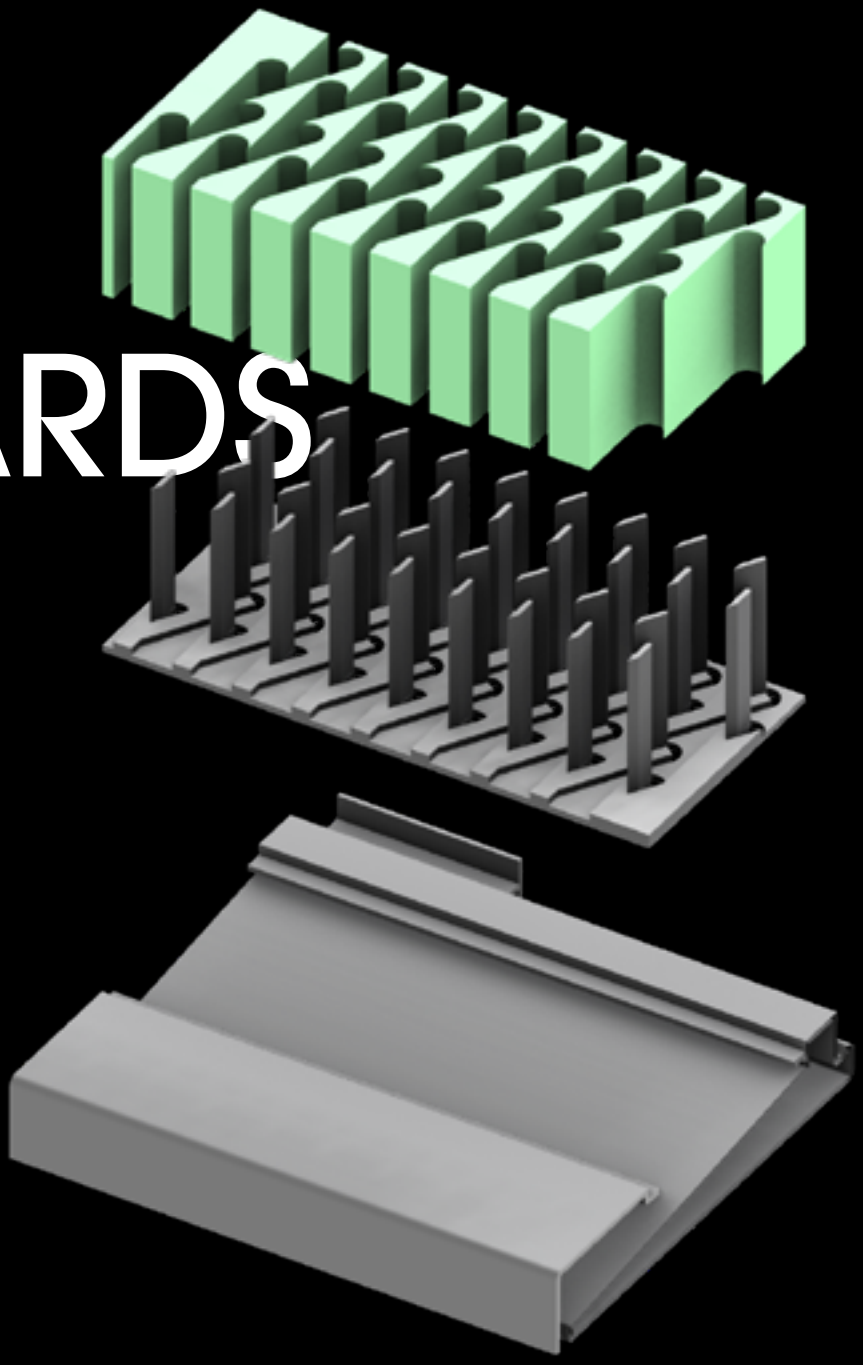

Section 12

design proposal & feasibility

There are many ways of integrating multiple elements and functions into a BV.

The FDP owns its internal structure to its main function, which is to regulate airflow. For this purpose, it uses Tesla valves. After having analyzed what other functions FDPs should have, and what passive solutions there are to do so, this chapter will see if these functions and geometry show overlap, and how they might be integrated into a holistic BV, using 3DP when needed. Apart from function, there are other factors at play. As discussed, the FDP is interesting in particular for its ability to be shaped into any form. On top of that, for optimal performance, the valves ought to be optimized for each particular application. Maintaining this degree of customization can almost only feasibly be done by 3DP. However, this does mean the production speed will be severely limited, and all other functions the FDP should have to make it multi-functional would have to be integrated by geometric, printable, and easy-to-integrate solutions. This might be possible, but such levels of complexity might make the 3D printing of the FDP unreasonably complex. This chapter will propose and compare other manufacturing methods for FDPs and propose a possible solution that allows the mass production of FDPs

12.1 functionalities

12.1.1 regulation

regulation is done with the FDP, but question if 3DP is the most suitable form. In its current form, it is a simple extrusion. There are methods more suitable to produce such shapes with a higher throughput. Additionally. not using 3D printing for the FDP, allows for the use of a larger variety of materials, which can perform a double function.

12.1.2 accoustics

This double function is most critically decided by the findings in chapter 10.2 where it was found that the area of the FDP has to be larger than that of a traditional BV. This means that either the entire design will have to be larger in diameter, or the acoustic lining will be removed to acquire the required free area. However, this does mean the FDP will have to offer very high sound insulation. This can be done by making the FDP out of a sound-absorbing material, as was proposed in chapter 10.2. There are many such foams, but many of them are not recyclable. However, bio-foam has the official cradle-to-cradle therefore resilient and behaves like ..., making it easy to process and suitable as a sound-absorbing material. Apart from the FDP performing a double function by creating it out of foam, it also means it can be produced significantly faster. Two methods qualify to do so, which are foam die-cutting processes Veinas, 2022 and industrial hot wire cutting MegaPlot, 2022.

12.1.3 filtering

Cao et al. (2020) (Cao et al., 2020) already mentioned filtering needed to be applied. But adding a filter to the FDP would increase its resistance even further which is undesired (Daniël, 2021). A simple solution would be to turn the FDP 90 degrees. As such, particles will fall to the bottom. In this configuration, the

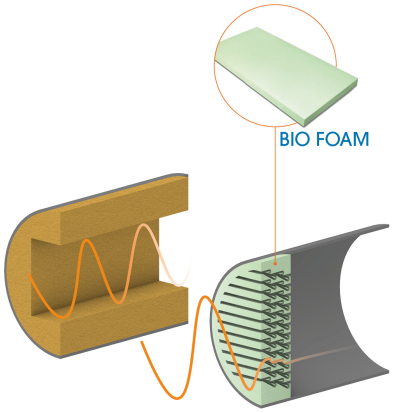

Figure 14: Since the FDP requires a larger are to allow for enough air to pass, implementing acoustic lining is no longer possible (without enlarging the entire inlet). Therefore it would be necessary to integrate the acoustic absorption into the FDP, potentially by making it out of an absorbing foam.

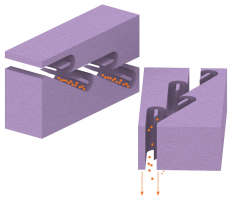

Figure 15: Rotating the valves ensures the dirt will fall to the bottom, where it can be disposed of or collected

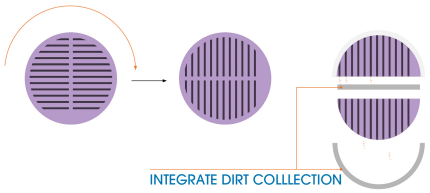

Figure 16: In the scenario of a circular FDP, dirt collection might be integrated into the rims

FDP might even function as a cyclone separator (Albanes et al., 2022), and smart design could improve this effect. In any case, this does mean that dirt will have to be collected and disposed of or stored which could be done in the lower rim.

12.2 Design

To turn these solutions into a functional design, one that could be incorporated into a trickle ventilator. As a reference, the Duco Skymax was chosen (Duco, 2024b). The design proposes an FDP out of bio-foam, manufactured using die-cutting (figure 9). The foam components can be held together by the rims without the need for any adhesives. How this might be achieved is explained in figure 10. Holes in the rim allow the disposal of the particles out of the valves and into a sloping compartment, integrated into the extrusion profile of the trickle ventilator, which in turn leads the particles to the outside. As such, the rims and baffles form a complex and multi-functional geometry which lends itself well for 3D printing.

12.3 Further improvements

The design does not solve all issues with NV. For example, heat loss still occurs. However, for such problems, we should perhaps look at behavioral changes instead, and find more efficient manners of heating that do not require the (inherently inefficient) heating of entire rooms, floors and buildings [low tech]. In general, technology will only bring us closer to our goal of a net zero built environment if the social-economical context in which it is deployed changes drastically (De Decker, 2023). Another problem is that cold drafts, and therefore thermal discomfort might persist. Further development of the product might result in manners to use of the baffles as pre-heating elements, such as the ones Duco integrated into their ClimaTop design (Groothoff, 2013), providing even more functionality to the FDP, but as such also complicating it significantly (Craig & Grinham, 2017), which does not fit in with the objective of this thesis.

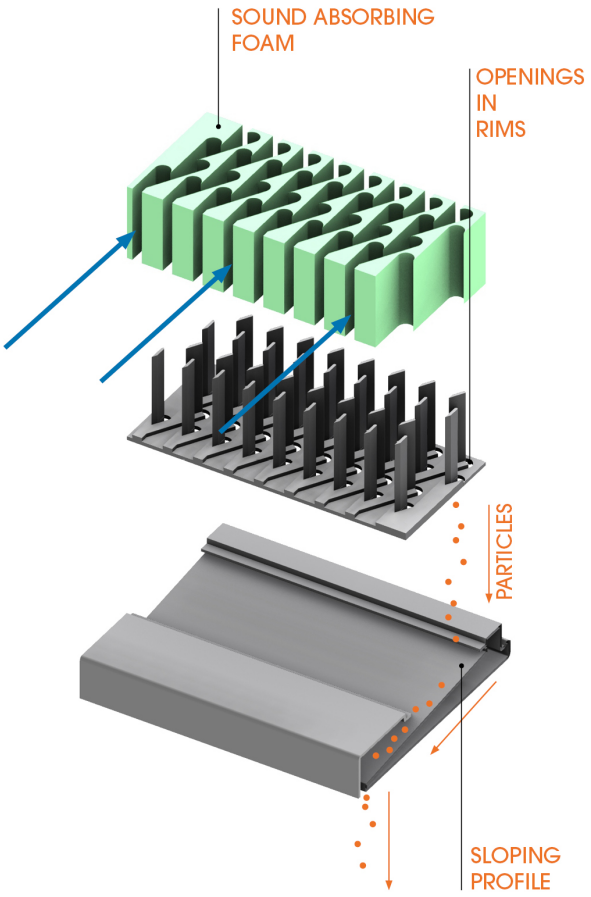

Figure 17: The complete functionality of the integrated FDP

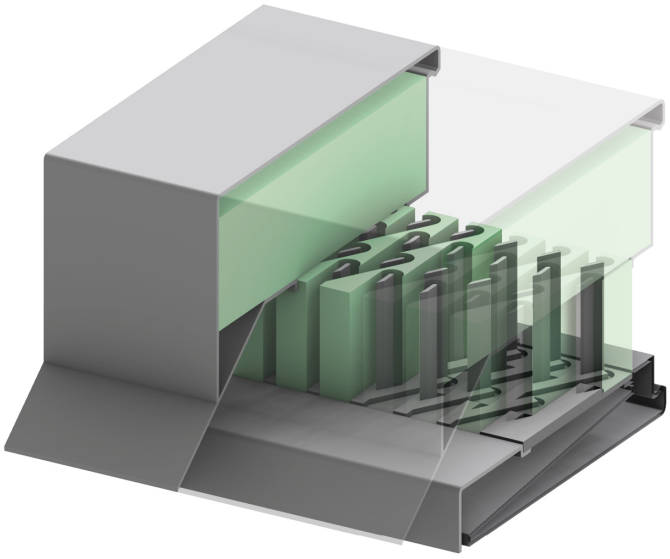

Figure 8: Complete integration of the FDP into the trickle ventilator

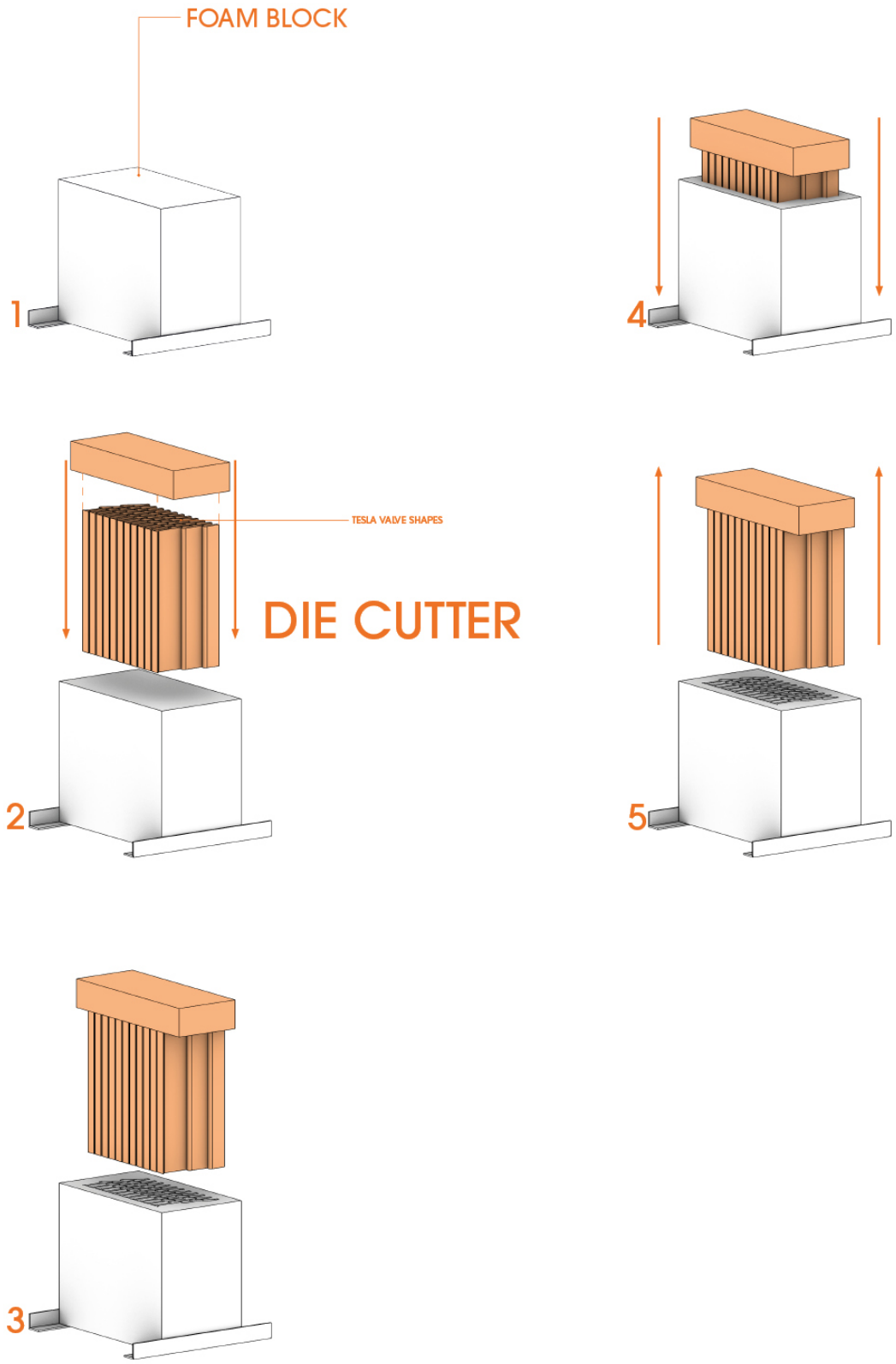

Figure 9: The process of die cutting the foam

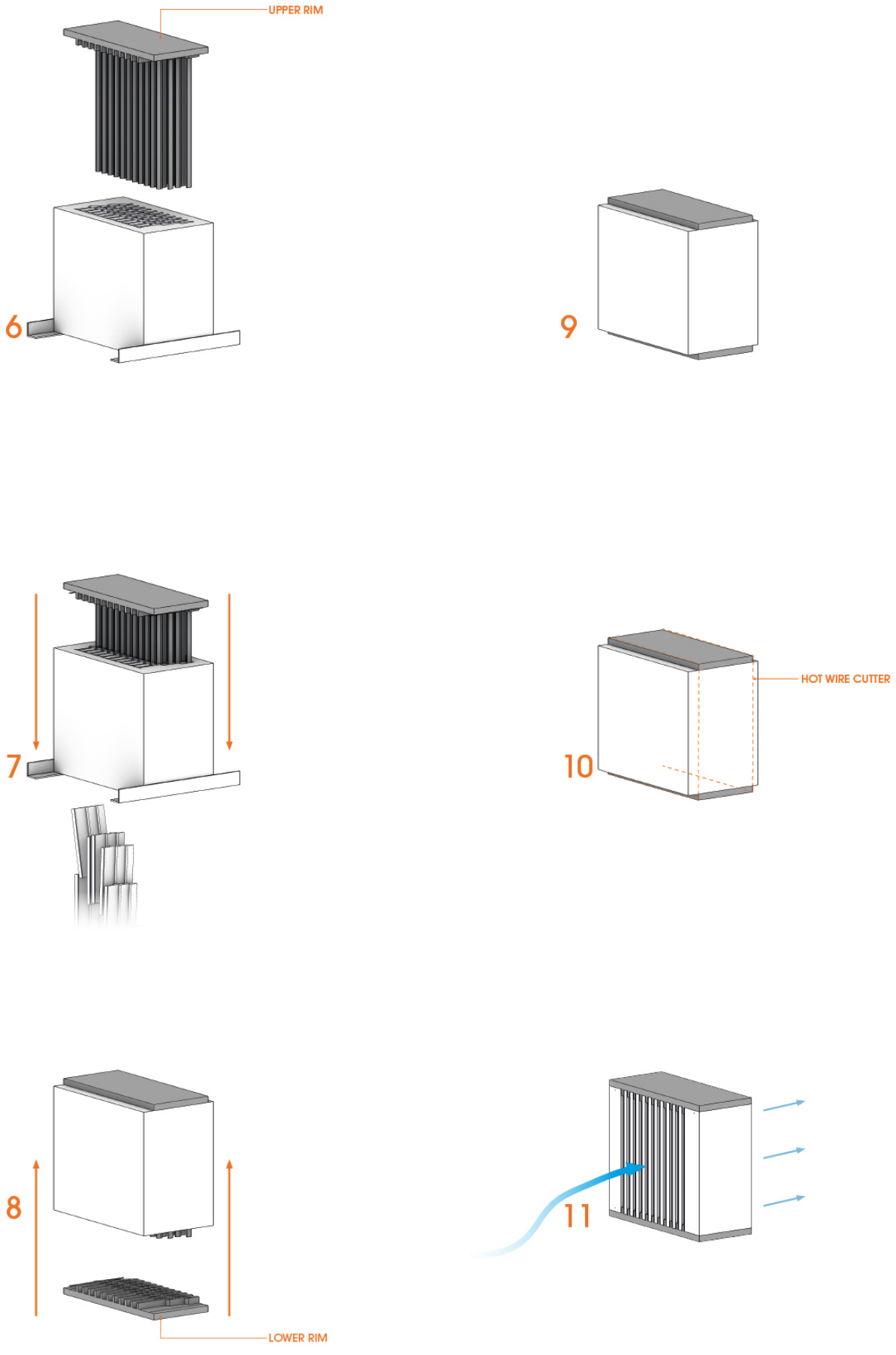

Figure 10: The assembly sequence of the foam and the rims

Section 13

Final Conclusion

The second part of the thesis served as a case study, by taking existing research into 3D printed components which complied with the requirements set in the first part for promising 3DP applications, and researching how it might be turned into a feasible and scalable product. Firstly, it discussed the basic principles of natural ventilation, its stringent design requirements to function, and the contradictory measures that have to be taken to tackle issues concerning sufficient airflow, thermal and acoustic comfort, and filtering. It is exactly this complexity that might be solved by a holistic and multi-functional 3D printed solution [SQ-V & SQ-VI]. Currently, trickle ventilators and background ventilators can solve some of these issues, but none of the solutions is ideal, and especially when it comes to the regulation of inflow, current solutions are either not sufficient or complex, which does not comply with the requirements for resilience. Therefore, special attention was given to the concept of fluid diode plates (FDPs) [SQ-VII]. Through literature research, it researched how FDPs could be applied in practice, revealing that their functionality might indeed be deployed efficiently to regulate inflow, but that a larger surface area is required compared to other background ventilators. However, this increase can be compensated if the FDP supplies acoustic insulation, making the need for acoustic lining in background ventilators redundant, meaning overall the surface area of the inlets can remain the same. This is however most easily achieved when the FDP is made of foam, meaning it can not be produced through AM. However, other parts were identified where 3DP could be deployed and adhere to the requirements for efficient 3DP design set in part one of this thesis, such as avoiding assembly steps [SQ-VIII]. Additionally, the use of 3DP was found to be promising for integrating low-frequency sound absorption and filtering in the BV design [SQ-IX].

> How can a shift towards a more holistic design approach facilitate the widespread adoption of additive manufacturing in the built environment, addressing immediate industry needs and fostering innovation and growth?

The first part identified immediate needs in the building industry such as carbon reduction, resilience, circularity, health, and equity, and highlighted the importance of scalable and simple solutions for accelerating refurbishment efforts, particularly in the European Union. Especially passive solutions such as 3D printed facades, acoustic dampeners, air filters, and regulators, integrated into holistic design were shown to both contribute towards this cause and are able to exploit the inherent capabilities of 3DP, including customization, multi-functionality, and the ability to create designs that are challenging to manufacture traditionally.

The second and third parts of the thesis served as a case study on natural ventilation, a complex issue that aligns with the goals of resilience and refurbishment. It discussed the multifaceted challenges of designing for adequate airflow, thermal comfort, and noise reduction while maintaining filtering capabilities. The potential of fluid diode plates (FDPs) was examined in detail, demonstrating how their enhanced functionality could address airflow regulation and acoustic insulation simultaneously, thereby reducing the complexity and amount of components compared to traditional methods.

The case study underscored the effectiveness of 3DP in creating multi-functional, integrated solutions that could lead to the redesign of existing components and systems in the building industry. By avoiding assembly steps and employing designs that

use the strengths of 3DP to integrate multiple functions into a single component, the adoption of 3DP technologies can be accelerated. This approach not only addresses the immediate needs of the industry but also promotes sustainability and innovation, suggesting a promising pathway for the future of construction and architectural design.

Ultimately, the shift towards a more holistic design approach in additive manufacturing can indeed facilitate its widespread adoption in the built environment, effectively addressing immediate industry needs while fostering innovation and growth. This approach not only meets current requirements but also sets a foundation for future advancements in building technologies.

Section 14

Reflection

14.0.1 methodology and relevance

The objective of this thesis was to establish a critical overview of the strengths and weaknesses of additive manufacturing in the context of the built environment and explore how these strengths and limitations influence the design process of mass-produced 3D printed solutions in the construction sector, with a particular focus on its potential to increase resilience in the built environment, which is an import consideration in the context of current societal and climate-related predicaments. To achieve this, an approach was chosen that was twofold. The first part of the research focused critically on the current applications of additive manufacturing in the built environment and asses its feasibility. It was concluded that for 3D printing to be a feasible manufacturing method, it has to be deployed to solve multi-faceted problems by producing complex, multi-functional parts that solve multiple problems at once. It was then concluded that this was most likely to be achieved in the field of climate design, as it was identified that such multi-dimensional problems were most common in the field of climate design. On top of that, research into 3D printing in the fields of structural and facade design was found to be plentiful and well-established. After identifying potential research directions within climate design, it was concluded that for the objective of this paper, natural ventilation, and in particular the role of background ventilators and how they could be improved using 3D printed fluid diode plates, filters and acoustic solutions, was the most promising direction to research further as a case study for the second part of the research, which focused on outlining how the strengths and weaknesses of 3D printing influence the design process. The second part of the thesis thus focused on understanding the passive and 3D printable methods available to improve background ventilators. Most of the research focused on the fluid diode plates, as research on them is scarce. Based on the results, the thesis proposed an optimization and selection method for the FDPs, so that the FDP can be generated to meet the needs of any specific case. At the same time, the optimal production method was explored, as well as a proposal on integrating the FDPs into a multi-functional background ventilator. This approach to the thesis was sufficient to the initial objective of the paper, namely to explore the consequences of the characteristics of 3D printing as a manufacturing method for mass-produced components. It led to the conclusion that to make 3D printing feasible, a holistic approach to the design process of building components had to be adapted, which was confirmed by existing literature. On the other hand, due to the broad nature of the thesis, the research stayed somewhat superficial, meaning that many of the ideas and concepts that were introduced will have to be tested and validated.

Assessing the academic and societal impact of the thesis, it can be concluded that 3D printing can play an important role in making the built environment more passive and therefore more resilient. However, it remains a complicated way of manufacturing, as the poor scalability of the technology remains a problematic issue. Therefore, the exploration of holistic design thinking to unlock 3D printing is an important consideration that came forth from this thesis. Additionally, successful improvement of background ventilators through resilient, 3D printed solutions might guarantee many, especially those in less wealthy countries, access to affordable, healthy, and quiet ventilation, which aligns with the qualifications set in the first part of this thesis as to what exactly counts as is societal value and innovation.

14.1 Personal

My aim with this thesis was not only to develop a relevant, scalable product but also to do so in a way that aligns with my values, which are that of aiming for low-tech, resilient solutions that might help improve the life of everyone with as little complexity as possible. As a Building Technology student, I often feel as if the opposite is oftentimes encouraged, namely to create convoluted solutions with little relevant impact. With this as a starting point, my research led me to discover many interesting aspects of design. What was most influential for the final design decisions was researching the concrete implications of what it means to design in a resilient manner. The technological solutions followed automatically, in large part thanks to my supportive professors, who encouraged me to maintain my critical attitude and provided me with essential insights into existing technologies and approaches. I think any engineer would benefit from following a similar approach to design, formulating critically what the social objectives of the design should be, and letting that guide the innovation. This thesis has shown that in doing so, it might happen that to innovate, high-tech solutions are not always required. This has led me to formulate the question 'What counts as innovation' and how might we make engineers and designers more aware that designing for resilience is not the same as relying on the latest technologies. For me personally at least, this thesis has been a first step into understanding that.

References

Acoustics & Noise Consultants. (2020). *Acoustics, ventilation and overheating residential design guide*. Retrieved January 22, 2024, from https://www.association-of-noise-consultants.co.uk/wp-content/uploads/2019/12/ANC-AVO-Residential-Design-Guide-January-2020-v1.1-1.pdf

Albanes, E., Biskos, G., Costi, M., & Biskos, G. (2022). Performance evaluation of a 3d-printed sharp-cut cyclone. *Environmental Science. Processes & Impacts*, *24*(8), 1173–1180. https://doi.org/10.1039/d2em00089j

Amfg. (2020, October 14). *10 of the biggest challenges in scaling additive manufacturing for production in 2020 [expert roundup]*. https://amfg.ai/2019/10/08/10-of-the-biggest-challenges-in-scaling-additive-manufacturing-for-production-expert-roundup/

Bao, Y., & Wang, H. (2022). Numerical study on flow and heat transfer characteristics of a novel tesla valve with improved evaluation method. *International Journal of Heat and Mass Transfer*, *187*, 122540. https://doi.org/10.1016/j.ijheatmasstransfer.2022.122540

Barnett, N., Costenaro, D., & Rohmund, I. (2017). *Direct and indirect impacts of robots on future electricity load* (tech. rep.). ACEEE.

Berardi, U., & Iannace, G. (2015). Acoustic characterization of natural fibers for sound absorption applications. *Building and Environment*, *94*, 840–852. https://doi.org/10.1016/j.buildenv.2015.05.029

Biler, A., Tavil, A., Su, Y., & Khan, N. (2018). A review of performance specifications and studies of trickle vents. *Buildings*, *8*(11), 152. https://doi.org/10.3390/buildings8110152

Böhm, S., Phi, H. B., Moriyama, A., Runge, E., Strehle, S., König, J., Cierpka, C., & Dittrich, L. (2022). Highly efficient passive tesla valves for microfluidic applications. *Microsystems & Nanoengineering*, *8*(1). https://doi.org/10.1038/s41378-022-00437-4

Buswell, R., Soar, R., Gibb, A., & Thorpe, T. (2005). The potential of freeform construction processes. *ResearchGate*. https://www.researchgate.net/publication/265994659_The_potential_of_freeform_construction_processes

Buswell, R. A., Soar, R., Gibb, A. G., & Thorpe, T. (2007). Freeform construction: Mega-scale rapid manufacturing for construction. *Automation in Construction*, *16*(2), 224–231. https://doi.org/10.1016/j.autcon.2006.05.002

Cambonie, T., Mbailassem, F., & Gourdon, E. (2018). Bending a quarter wavelength resonator: Curvature effects on sound absorption properties. *Applied Acoustics*, *131*, 87–102. https://doi.org/10.1016/j.apacoust.2017.10.004

Can, A., Leclercq, L., Lelong, J., & Botteldooren, D. (2010). Traffic noise spectrum analysis: Dynamic modeling vs. experimental observations. *Applied Acoustics*, *71*(8), 764–770. https://doi.org/10.1016/j.apacoust.2010.04.002

Cao, Z., Zhao, T., Wang, Y., Wang, H., Zhai, C., & Lv, W. (2020). Novel fluid diode plate for use within ventilation system based on tesla structure. *Building and Environment*, *185*, 107257. https://doi.org/10.1016/j.buildenv.2020.107257

Castaño-Rosa, R., Pelsmakers, S., Järventausta, H., Poutanen, J., Tähtinen, L., Rashidfarokhi, A., & Toivonen, S. (2022). Resilience in the built environment: Key characteristics for solutions to multiple crises. *Sustainable Cities and Society*, *87*, 104259. https://doi.org/10.1016/j.scs.2022.104259

Catapane, G., Petrone, G., Robin, O., & Verdière, K. (2023). Coiled quarter wavelength resonators for low-frequency sound absorption under plane wave and diffuse acoustic field excitations. *Applied Acoustics*, *209*, 109402. https://doi.org/10.1016/j.apacoust.2023.109402

Cauberg, J. (2005, August). *Natuurlijke ventilatie en infiltratie*. https://klimapedia.nl/module/natuurlijke-ventilatie-en-infiltratie/

Cauberg, J. (2013). *Drukverschillen over scheidingsconstructies* (Tech. Report No. Kennisbank Bouwfysica Dictaat ct 4220 Bouwfysica II). TU Delft, Faculteit Civiele Techniek en Geowetenschappen. https://klimapedia.nl/wp-content/uploads/2013/05/LU_11_drukverschillen_over_scheidingsconstructies.pdf

Craig, S., & Grinham, J. (2017). Breathing walls: The design of porous materials for heat exchange and decentralized ventilation. *Energy and Buildings*, *149*, 246–259. https://doi.org/10.1016/j.enbuild.2017.05.036

Daniël, D. (2021). *Reducing the indoor exposure to traffic emissions: Study and concept design of air purification systems for the façades of high-rise buildings in industrialized urban environments*. %5Curl%7Bhttps://repository.tudelft.nl/islandora/object/uuid:05813c2b-75dc-4c15-bfae-1dee9075157a?collection=education%7D

De Decker, K. (2023). Thematic book series: Heating people, not spaces [Accessed: 2024-06-17]. *LOWTECH MAGAZINE*. https://solar.lowtechmagazine.com/2023/12/thematic-book-series-heating-people-not-spaces/

De Salis, M. H. F., Oldham, D., & Sharples, S. (2002). Noise control strategies for naturally ventilated buildings. *Building and Environment*, *37*(5), 471–484. https://doi.org/10.1016/s0360-1323(01)00047-6

Du, G., Alsenani, T. R., Kumar, J., Alkhalaf, S., Alkhalifah, T., Alturise, F., Almujibah, H., Znaidia, S., & Deifalla, A. (2023). Improving thermal and hydraulic performances through artificial neural networks: An optimization approach for tesla valve geometrical parameters. *Case Studies in Thermal Engineering*, *52*, 103670. https://doi.org/10.1016/j.csite.2023.103670

Duco. (2024a). Silenzio zr (ak).

Duco. (2024b). Skymax zr [Accessed: 2024-06-17].

Eco traject. (2016). *Slimme technieken ventilatiesysteem c*. https://cdn.nimbu.io/s/4tn7vz5/assets/5.2.1%20Technieken%20-%20ventilatiesysteem%20C.pdf

El-Sayegh, S. M., Romdhane, L., & Manjikian, S. (2020). A critical review of 3d printing in construction: Benefits, challenges, and risks. *Archives of Civil and Mechanical Engineering*, *20*(2). https://doi.org/10.1007/s43452-020-00038-w

Engineeringtoolbox. (2024a). Air duct components - minor dynamic loss coefficients. Retrieved April 12, 2024, from https://www.engineeringtoolbox.com/minor-loss-air-ducts-fittings-d_208.html

Engineeringtoolbox. (2024b). Fluid flow - hydraulic diameter. Retrieved April 23, 2024, from https://www.engineeringtoolbox.com/hydraulic-equivalent-diameter-d_458.html
European Parliament. (2023). Energy performance of buildings [Geraadpleegd op 28 januari 2024].
Fadl, A., Zhang, Z., Geller, S., Tölke, J., Krafczyk, M., & Meyer, D. (2009). The effect of the microfluidic diodicity on the efficiency of valve-less rectification micropumps using lattice boltzmann method. *Microsystem Technologies*, *15*(9), 1379–1387. https://doi.org/10.1007/s00542-009-0901-7
Federation of European HVAC associations [REHVA]. (2012). *Existing buildings, building codes, ventilation standards and ventilation in europe* (tech. rep.) (Retrieved January 22, 2024). REHVA. https://www.rehva.eu/fileadmin/EU_projects/HealthVent/HealthVent_WP5_-_Final_Report.pdf
Field, C. (2004–August 25). The latest developments of an attenuator for naturally ventilated buildings. *Proceedings of the 33rd International Congress and Exposition on Noise Control Engineering*. https://www.researchgate.net/publication/308973203_The_Latest_Developments_of_an_Attenuator_For_Naturally_Ventilated_Buildings
Filamentives. (n.d.). How sustainable is pla 3d printer filament?
Formlabs. (n.d.). Guide to resin 3d printers: Sla vs. dlp vs. msla vs. lcd.
Formlabs. (n.d.). 3d printing technology comparison: Fdm vs. sla vs. sls. https://formlabs.com/eu/blog/fdm-vs-sla-vs-sls-how-to-choose-the-right-3d-printing-technology/
Ganji, D., & Kachapi, S. H. H. (2015). Natural, mixed, and forced convection in nanofluid. In *Elsevier ebooks* (pp. 205–269). https://doi.org/10.1016/b978-0-323-35237-6.00006-6
Gebler, M., Uiterkamp, A. J. M. S., & Visser, C. (2014). A global sustainability perspective on 3d printing technologies. *Energy Policy*, *74*, 158–167. https://doi.org/10.1016/j.enpol.2014.08.033
Ghaffar, S. H., Corker, J., & Fan, M. (2018). Additive manufacturing technology and its implementation in construction as an eco-innovative solution. *Automation in Construction*, *93*, 1–11. https://doi.org/10.1016/j.autcon.2018.05.005
Gibson, I., Rosen, D. W., Stucker, B., & Khorasani, M. (2020). Design for additive manufacturing. In *Springer ebooks* (pp. 555–607). https://doi.org/10.1007/978-3-030-56127-7_19
Griffin, M. (2024, February). Is 3d printer resin toxic? all you need to know.
Groothoff, M. (2013). Duco climatop: Slimme ventilatie, ultiem comfort [Accessed: 2024-06-17]. *Glas in Beeld*. https://www.glasinbeeld.nl/7266/duco-climatop-slimme-ventilatie-ultiem-comfort/
Healthy Buildings Program. (2017). *The 9 foundations of a healthy building* (tech. rep.). HBP. https://forhealth.org/9_Foundations_of_a_Healthy_Building.February_2017.pdf
Hickel, J. (2021). *Less is more*. Windmill Books.
Hinchy, E. P. (2019). Design for additive manufacturing. In *Springer ebooks* (pp. 23–50). https://doi.org/10.1007/978-3-030-24532-0_2
Hu, H., Son, I., Kikumoto, H., Zhang, B., & Hayashi, K. (2024). Improving tesla valve shape within fluid diode plates for building ventilation. *Building and Environment*, *252*, 111259. https://doi.org/10.1016/j.buildenv.2024.111259
Huston, M. (2024). *Architecture and the environmental impact of artificial complexity*. Retrieved May 6, 2024, from https://www.archdaily.com/957549/architecture-and-the-environmental-impact-of-artificial-complexity
International Energy Agency. (2021). Net zero by 2050 [License: CC BY 4.0].
International Energy Agency. (2022, September). Renovation of near 20% of existing building stock to zero-carbon-ready by 2030 is ambitious but necessary – analysis.
International Energy Agency. (2023). *Tracking clean energy progress 2023* (tech. rep.) (License: CC BY 4.0 via: https://www.iea.org/energy-system/buildings). IEA. Paris. https://www.iea.org/reports/tracking-clean-energy-progress-2023
International Energy Agency (IEA). (2022). Technology and innovation pathways for zero-carbon-ready buildings by 2030 [Licence: CC BY 4.0].
Jared, B. H., Aguiló, M. A., Beghini, L. L., Boyce, B., Clark, B. W., Cook, A., Kaehr, B., & Robbins, J. (2017). Additive manufacturing: Toward holistic design. *Scripta Materialia*, *135*, 141–147. https://doi.org/10.1016/j.scriptamat.2017.02.029
Khajavi, S. H., Tetik, M., Mohite, A., Peltokorpi, A., Li, M., Weng, Y., & Holmström, J. (2021). Additive manufacturing in the construction industry: The comparative competitiveness of 3d concrete printing. *Applied Sciences*, *11*(9), 3865. https://doi.org/10.3390/app11093865
Kim, K., Park, K., & Jeon, H.-W. (2022). The impact of design complexity on additive manufacturing performance. *IFIP Advances in Information and Communication Technology*, 227–234. https://doi.org/10.1007/978-3-031-16407-1_27
Leschok, M., Cheibas, I., Piccioni, V., Seshadri, B., Schlueter, A., Gramazio, F., Köhler, M., & Dillenburger, B. (2023). 3d printing facades: Design, fabrication, and assessment methods. *Automation in Construction*, *152*, 104918. https://doi.org/10.1016/j.autcon.2023.104918
Liu, Z., Shao, W., Sun, Y., & Sun, B. (2022). Scaling law of the one-direction flow characteristics of symmetric tesla valve. *Engineering Applications of Computational Fluid Mechanics*, *16*(1), 441–452. https://doi.org/10.1080/19942060.2021.2023648
McNeel. (n.d.). Compute.rhino3d/src/ghhops-server-py [https://github.com/mcneel/compute.rhino3d/tree/8.x/src/ghhops-server-py].
MegaPlot. (2022, November). Xtr pro abrasive fast wire foam cutting machines [Accessed: 2024-06-17].
Mocz, P. (2022, November). *Create your own lattice boltzmann simulation (with python)*. Medium. https://medium.com/swlh/create-your-own-lattice-boltzmann-simulation-with-python-8759e8b53b1c
NEN. (2013). *Bouwbesluit ventilatie* (tech. rep.). Nederlands Normalisatie-instituut.
Neutrium. (n.d.). Hydraulic diameter [Neutrium. Accessed on: 23/04/2024]. https://neutrium.net/fluid-flow/hydraulic-diameter/

Niaki, M. K., Torabi, S. A., & Nonino, F. (2019). Why manufacturers adopt additive manufacturing technologies: The role of sustainability. *Journal of Cleaner Production*, *222*, 381–392. https://doi.org/10.1016/j.jclepro.2019.03.019
Nijeboer & Hage. (n.d.). *Drukverschillen bij natuurlijke ventilatie, type c* (Tech Report). https://www.duco.eu/Wes/CDN/1/Attachments/Notitie%20drukverschil%20bij%20natuurlijk%20ventileren_3_635984962745408705.pdf
Ortiz, M. (2022, April). Simple lattice-boltzmann simulator in python | computational fluid dynamics for beginners. https://www.youtube.com/watch?v=JFWqCQHg-Hs
Peels, J. (2023, October). RIP 3D Printing: 1987 2023, Complexity is Expensive [3DPrint.com | the Voice of 3D Printing / Additive Manufacturing].
Peng, C., Xu, J., Kumar, J., Almujibah, H., Ali, H., Alkhalifah, T., Alkhalaf, S., Alturise, F., & Ghandour, R. (2023). Improving efficiency and optimizing heat transfer in a novel tesla valve through multi-layer perceptron models. *Case Studies in Thermal Engineering*, *49*, 103391. https://doi.org/10.1016/j.csite.2023.103391
Pleysier, I. A., & Vos, M. (2017). Luchttransport door constructies. %5Curl%7Bhttps://klimapedia.nl/wp-content/uploads/2017/07/WV952-H6-Luchttransport-2016-2017-v1.0.pdf%7D
Pradel, P., Bibb, R., Zhu, Z., & Moultrie, J. (2017). Complexity is not for free: The impact of component complexity on additive manufacturing build time. *ResearchGate*. https://www.researchgate.net/publication/327424268_Complexity_is_not_for_free_the_impact_of_component_complexity_on_additive_manufacturing_build_time
Purwidyantri, A., & Prabowo, B. A. (2023). Tesla valve microfluidics: The rise of forgotten technology. *Chemosensors*, *11*(4), 256. https://doi.org/10.3390/chemosensors11040256
Rashid, A. A., Al-Ghamdi, S. G., & Koç, M. (2020). Additive manufacturing: Technology, applications, markets, and opportunities for the built environment. *Automation in Construction*, *118*, 103268. https://doi.org/10.1016/j.autcon.2020.103268
Rijksgebouwendienst, Bureau Bouwfysica, Afdeling Onderzoek en Ontwikkeling. (1984, February). *Uitgangspunten bij de vaststelling van de aan de luchtdoorlatendheid van gevels te stellen eisen* (Internal Report). Rijksgebouwendienst. 's-Gravenhage.
Schork, T., Titchkosky, N., Bickerton, C., Reinhardt, D., Bennett, M., Pigram, D., & Makki, M. (2021). The geometry of air: Large-scale multi-colour robotic additive fabrication for air-diffusion systems. *Construction Robotics*, *5*(1), 49–61. https://doi.org/10.1007/s41693-021-00054-z
Setaki, F., Tian, F., Turrin, M., Tenpierik, M., Nijs, L., & Van Timmeren, A. (2023). 3d-printed sound absorbers: Compact and customisable at broadband frequencies. *Architecture, Structures and Construction*, *3*(2), 205–215. https://doi.org/10.1007/s44150-023-00086-9
SimScale. (2023, November). The lattice boltzmann method (lbm) in cfd | simwiki | simscale [Retrieved on January 22, 2024].
Solidator. (2023, December). Msla - what are the advantages of msla over sla? solidator resin 3d printer. https://solidator.com/en/msla-sla-comparison/
Strau, H. (2017). Am envelope. the potential of additive manufacturing for facade constructions. *DOAJ (DOAJ: Directory of Open Access Journals)*. https://doi.org/10.7480/abe.2013.1
Tang, S. K. (2017). A review on natural ventilation-enabling façade noise control devices for congested high-rise cities. *Applied Sciences*, *7*(2), 175. https://doi.org/10.3390/app7020175
TCPoly. (2021). PANELTM FOR HEAT RECOVERY IN COMMERCIAL BUILDINGS.
Tedeschi, A. (2014). *Aad algorithms-aided design | parametric strategies using grasshopperő*. Edizioni Le Penseur - Le Penseur Publisher. https://www.lepenseur.it/books-and-training/aad-algorithms-aided-design-parametric-strategies-using-grasshopper/
Vaferi, K., Vajdi, M., Shadian, A., Ahadnejad, H., Moghanlou, F. S., Nami, H., & Jafarzadeh, H. (2023). Modeling and optimization of hydraulic and thermal performance of a tesla valve using a numerical method and artificial neural network. *Entropy*, *25*(7), 967. https://doi.org/10.3390/e25070967
van Herpen, R. (2005, August). Meerzone luchtstroommodellen.
Veinas. (2022, April). Veinas epe foam machine [Accessed: 2024-06-17]. https://www.youtube.com/watch?v=DxjhrAQGdHI
Volkshuisvesting en Ruimtelijke Ordening. (2022). Beleidsprogramma versnelling verduurzaming gebouwde omgeving [Geraadpleegd op 28 januari 2024].
Weger, D., Gehlen, C., Korte, W., Meyer-Brötz, F., Scheydt, J. C., & Stengel, T. (2021). Building rethought 3d concrete printing in building practice. *Construction Robotics*, *5*(3–4), 203–210. https://doi.org/10.1007/s41693-022-00064-5
World Green Building Council. (2023). *Global policy principles for a sustainable built environment* (tech. rep.). World Green Building Council. https://worldgbc.org/wp-content/uploads/2023/04/WorldGBC-Global-Policy-Principles_FINAL.pdf
Wu, P., Wang, J., & Wang, X. (2016). A critical review of the use of 3-d printing in the construction industry. *Automation in Construction*, *68*, 21–31. https://doi.org/10.1016/j.autcon.2016.04.005
Yin, H., Qu, M., Zhang, H., & Lim, Y. (2018). 3d printing and buildings: A technology review and future outlook. *Technology Architecture + Design*, *2*(1), 94–111. https://doi.org/10.1080/24751448.2018.1420968
Zhang, Y., Tong, J., & Zhu, Z. (2023). Numerical calculation of forward and reverse flow in tesla valves with different longitudinal width-to-narrow ratios. *Scientific Reports*, *13*(1). https://doi.org/10.1038/s41598-023-39758-3
Zhu, J., Zhou, H., Wang, C., Lü, Z., Yuan, S., & Zhang, W. (2021). A review of topology optimization for additive manufacturing: Status and challenges. *Chinese Journal of Aeronautics*, *34*(1), 91–110. https://doi.org/10.1016/j.cja.2020.09.020